Removals of Polyethylene Terephthalate (PET) Nanoplastics from an Activated Sludge: Improvement of Yields by Ni-Cu-C Nanocomposite

RUKİYE ÖZTEKİN [a], DELİA TERESA SPONZA [a,*]
[a] Department of Environmental Engineering
Dokuz Eylül University
Tınaztepe Campus, 35160 Buca/Izmir,
TURKEY
* Corresponding Author

Abstract: - In this study, the maximum polyethylene terephthalate (PET) nanoplastics (NPs) removal efficiency was investigated under optimum conditions by using various experimental parameters to improve the removal efficiency by using Ni-Cu-C NCs in an activated sludge solution. The effect of increasing pH values (4.0, 5.0, 6.0, 7.0 and 8.0), increasing adsorption times (30 min, 60 min, 90 min and 120 min), different Ni-Cu-C NCs adsorbent concentrations (100 mg/l, 200 mg/l, 300 mg/l and 400 mg/l) and different PET NPs concentrations (1 mg/l, 5 mg/l, 10 mg/l and 15 mg/l) on the adsorption yields of PET NPs was investigated in an activated sludge process during adsorption process. The characteristics of the synthesized Ni-Cu-C NCs were assessed using XRD, FTIR, FESEM, EDX and HRTEM analyses. ANOVA statistical analysis was used for all experimental samples. In order to remove 10 mg/l PET NPs with yields as high 99.20% and 99.42% in an activated sludge process via adsorption; the Ni-Cu-C NCs adsorbent concentration, adsorption time, pH and temperature should be 300 mg/l, 120 min, 7.0 and at 25°C, respectively. Adsorption process; it is an easily applicable, environmentally friendly and economical method.

Key-Words: - Activated sludge; Adsorption; Adsorption isotherm; Adsorption kinetic; Adsorption mechanism; ANOVA statistical analysis; Nanoplastics; Nikel-copper-carbon nanocomposite (Ni-Cu-C NCs); Polyethylene Terephthalate (PET).

Received: March 24, 2024. Revised: August 16, 2024. Accepted: September 21, 2024. Published: November 29, 2024.

1 Introduction

Plastics are petrochemical-based organic polymers that can be converted into different shapes and sizes. The demand for plastics has been continuously increasing due to low cost, inertness, flexibility, resistance to oxidation and high durability among others and they have been used since a hundred years, [1-3], and will continue to increase in the future. Studies performed to detect the plastic enumeration showed that they will double in 20 years and almost quadruple by 2050, [4]. Approximately 76% of the total plastic production is treated as waste: 12% is burned, 79% is buried or released into the environment, and only 9% is recycled, [5]. The incineration of plastics causes the release of carbon monoxide, dioxins and dioxin-related intermediates, as well as nitrogen oxides, into the atmosphere. This situation causes air pollution and makes it very difficult to completely remove plastic waste from the ecosystem. Plastics are synthetic materials made up of polymers, which are long molecules around chains of carbons atoms, especially hydrogen, nitrogen, oxygen, and sulfur, [6]. Plastics can be categorized based on their size, i.e., microplastics (> 25 mm), mesoplastics (5–25 mm), microplastics (MPs) (0.1–5 mm), and nanoplastics (NPs) (< 100 nm), [7].

Nanoplastics (NPs) are caused by plastic contamination, which is a global environmental problem due to their persistence in the environment. Moreover, due to the poor degradability of NPs, they tend to exist for a long time in the environment. The widespread presence of NPs in environmental matrices is due to their undesirable effects on biodiversity of both terrestrial and aquatic ecosystems; are studied as the main vectors of toxic pollutants and their common causes. NPs also be associated with dangerous substances/agents, leading to potential risks. NPs can lead to a risk to the water environment by transporting pathogens and the desorption of toxic chemicals. Because NPs have a huge surface area and hydrophobicity, they can adsorb on their surfaces with various contaminated toxic/dangerous substances such as antibiotics agent, persistent organic pollutants (POPs), polycyclic

aromatic hydrocarbons (PAHs), heavy/toxic metals, polychlorinated biphenyls (PCBs) and become a new contaminant in wastewater. Several emerging contaminants, such as Bisphenol A, atrazine, perfluoro alkylates, etc., can impose harmful effects on biodiversity through their adsorption and desorption on NPs. If the emerging contaminant-loaded NPs invade the food chain through ingestion by biota, it will lead to potential hazards to human health and the ecosystem, [8]. The ingestion of NPs obstructs the digestive tract, inhibit growth, cause reproductive disorders, increase mortality of aquatic life forms like marine bivalves, microalgae, amphipods, etc., [9, 10]. So, it is necessary to set strict discharge standards for NPs and emphasize the development of advanced treatment technologies to minimize the quantity of NPs entering into different environmental components.

Plastics are used in a wide variety of sectors for example; packaging, building, transportation, renewable energy, medical devices or sport equipment. The most common plastic materials in commercial products found in effluents are polypropylene (PP), polyethylene (PE), polystyrene (PS), polyvinyl-chloride (PVC), polycarbonate (PC), polyamides (PA), polyester (PES) and polyethylene terephthalate (PET), depending on the type of products produced by the plant, [11, 12]. These are reversible thermoplastic polymers, highly recyclable materials that can be heated, cooled and shaped repeatedly, [11, 12]. These represent approximately 90% of world production, [11-14].

Polyethylene terephthalate (PET) is widely used in packaging materials for its excellent abrasive resistance, dimensional stability, and insulation, [15]. PET, like other thermoplastic polymers, such as Polyethylene (PE), Polypropylene (PP), Polystyrene (PS) and Polycarbonates (PC), can be recycled by melting through high temperature processes, and reintegrated into new products, [16, 17]. This recycling technology, however, consumes sizable amounts of energy and, upon melting, lower grade polymers are produced, with reduced thermal and mechanical stability, which limit the applicability of this technique to a reduced number of cycles, [18]. The chemical degradation of PET and other plastics into their constituents represents another industrial viable approach, [19]. Focusing on PET, 70 million tons of this plastic are annually produced worldwide, [20], underlining the necessity of developing effective recycling approaches for this polymer. PET is made up of building block monomers, such as terephthalic acid (or benzene-1,4-dicarboxylic acid, H_2BDC) and ethylene glycol, and it can be conveniently exploited as a source of organic ligands, [21, 22]. The use of PET has made our lives more convenient, but improper handling of PET has caused serious damage to the environment. Despite the existence of PET recycling processes, a considerable amount of PET inevitably enters the wastewater treatment plants (WWTPs), [23]. As a non–volatile solid, PET may adversely affect the rheological properties of sludge in WWTPs, and new industrial discharge processes in WWTPs have been proposed, [24, 25].

Some treatment technologies for the removal of nano/microplastics in water have been developed, including flocculation [26], ingestion by microbes [27], biofilter technology [28], chlorination [29], UV oxidation [30] and membrane filtration [31]. Different removal technologies based on adsorption mechanisms have been proven to be effective approaches to remove NPs in aquatic environments. The chemically synthesized sponge materials, [32-35], graphene materials, [36], and biochar materials, [37], can be used to remove NPs and NPs in natural waters. Filtration could also be applied to NPs removal in aquatic environments. The biofilter prepared by Kuoppamaki et al. not only removes nutrients and heavy metals in rainwater, but also remove NPs, [38]. In addition to adsorption and filtration, some other technologies also show excellent application prospects in the removal of NPs in the aquatic environment. Electrocoagulation (EC) removes NPs through a series of physical-chemical reactions, [39, 40]. In flocculation process, Lysozymeamyloid fibrils servesas a novel natural bio-flocculant for removing dispersed NPs from water, [41]. Enriched NPs can be combined with recycling technology to achieve harmless treatment of NPs. Also, Noncovalent interactions removal mechanism with pressure-sensitive adhesive removal technology, [42], collect and fuse NPs into large bulks in the microbubble with solar energy removal technology, [43], were applied for the removal of NPs from aquatic environments.

In WWTPs, the most frequently engaged secondary treatment technologies are biological processes, notably activated sludge processes (ASP), which rely on the activated microorganisms in the sludge to degrade/transform the NPs, [44-46]. At Fig. 1, was determined to the mechanism of sorption of NPs removal during ASP in WWTPs. Currently, the reported MPs removal methods in sludge are mostly based on the degradation of MPs by bacteria in activated sludge, but cannot be used as the mainstream technology because of the lower

efficiency. For example, the bacteria strain isolated from activated sludge degraded 17% of PET NPs of 2.63 g/l, which was incubated at 30°C under a pH=7.0-7.5 with a reactor residence time of 168 days, [47]. Hyper-thermophilic composting (hTC) technology was used for in situ degradation of MPs in sludge, hTC significantly enhanced biodegradation of sludge-based MPs and after 45 days of hTC treatment, 43.7% of the MPs were removed from the sewage sludge, which was the highest ever reported for MPs biodegradation, [48].

* Fig. 1 can be found in the Appendix section.

Adsorption is mainly classified into two types: physical adsorption and chemisorption (described as activated adsorption as well). Physical adsorption is the adhesion of an adsorbent to the surface of an adsorbate because of the nonspecific (such as independent of the nature of the material) van der Waals force, whereas chemisorption occurs while chemical bonding creates strong attractive forces, for example chemical adsorption constructs ionic or covalent bonds through chemical reactions. Nevertheless, physical adsorption is a reversible process but less specific, whereas chemisorption is irreversible but more specific, [49]. When adsorption occurs over biological systems, the process is referred to as biosorption. Biosorption is a process that combines metal removal and recovery. Biosorption is effective due to the adsorbents' low cost and ease of regeneration. Bacteria, fungi, algae, industrial waste, agricultural waste, natural residues, and other biological materials have all been widely used to adsorb heavy metals from wastewater, [50]. Physical adsorption, chemisorption, electrostatic interactions, simple diffusion, intra-particle diffusion, hydrogen bonding, redox interactions, complexation, ion exchange, precipitation, and pore adsorption are all possible mechanisms to adsorb heavy metal ions onto bio-adsorbents, [51, 52].

Different removal technologies based on adsorption mechanisms have been proven to be effective approaches to remove NPs in aquatic environments. The chemically synthesized sponge materials, [53-56], graphene materials, [57], and biochar materials, [58], can be used to remove NPs in natural waters. Many factors can also affect the NPs removal efficiency including pH, temperature, adsorbents types, dissolved organic matter (DOM), and ions, but pH and temperature are the two most important factors. pH affects the adsorption efficiency mainly by influencing the charge on the surface of NPs and the adsorbent. Temperature can affect the adsorbate diffusion rate and equilibrium capacity, and higher temperatures achieve more NPs adsorption, [56]. Different adsorbents types have different electrostatic and hydrogen bonding interactions with NPs, thereby altering the adsorption capacity. DOM changes the interaction of absorbents with NPs, [59]. On top of this, ions can influence the electrostatic attraction between NPs and the adsorbent, which in turn alters the NPs adsorption by adsorbent, [60, 61]. In other words, the adsorption removal of NPs has the advantages of high adsorption capacity, high removal efficiency, low energy consumption and reusability. However, the adsorbents need to be eluted from the adsorbed NPs after use, which allows for the potential risk that the NPs would re-enter the environment.

Adsorbent is a pollutant remover widely used in water treatment plants with the advantages of high efficiency, simple operation and environmental friendliness. Carbon-based adsorbents such as modified activated carbon (AC) and other carbonic materials (graphene oxide and carbon nanotubes) have received a lot of attention recently because of their high thermal and chemical stability, [62]. AC is the most commonly used adsorbent which is characterized by low cost, a large surface area, high thermal and chemical stability, high porosity, and a controllable pore size distribution, [63]. However, an AC adsorbent lacks functional groups, so its use in heavy-metal ion adsorption has been limited due to its low uptake and slow kinetics, [64]. Metal-organic framework carbon materials have been increasingly proposed in recent years as adsorbents for a wide range of applications. Metal-organic framework carbon materials have a large specific surface area and a large number of pores, which can effectively adsorb various pollutants, [65], and is also a very promising water purification material. Metal-organic framework carbon materials show excellent adsorption removal performance in the removal of heavy metals, [66, 67], the removal of pesticides, [68], and the removal of cesium and strontium, [69].

The studies performed with the removal of PET is limited with few recent studies: n some studies it was shown that the PET was converted to new shape nanocomposites. Soni et al., [70], prepared PET-based carbonaceous compounds using hydrothermal processes to investigate of PET waste conversion to carbonaceous materials. Sharifian et al., [71], prepared PET-based AC (PET-AC) to reuse the PET with homogeneous and heterogeneous porosity textures to separate some pollutants. Pasanen et al., [72], generated magnetic ZIF-8 nanoparticles (Nano-Fe@ZIF-8) for magnetic extraction and depolymerization of PET nanoplastics. The Zn(II) present in Nano-Fe@ZIF-8 subsequently acted as a

catalyst for the depolymerization of the PET nanoplastics using ethylene glycol. Zheng et al., [73], prepared carbon-based adsorbents, such as graphene, graphene oxide (GO), activated carbon/biochar (AC/BC), carbon nanotubes (CNTs) to detect their potential effectiveness in removing microplastics and nano-plastics like PET and vinyl alcohol from aqueous solutions. Kang et al., [74], developed a MoS_2/g-C_3N_4 photocatalyst that can cenvert the PET into valuable organic chemicals. Kang et al., [74], upcycled the PET plastic wastes into value-added chemicals by using a nickel (Ni)-based catalyst prepared via electrochemically depositing copper (Cu) species on Ni foam (NiCu/NF).

Bimetallic organic framework carbon materials are preferred because they have the ability to improve the stability and activity of the original materials, [75]. Copper (Cu) and nickel (Ni) have often been used to develop inefficient composite catalysts due to their good synergy, low cost, and high removal efficiencies, [75, 76]. Cu and Ni-based bimetallic organic framework carbon materials have been applied to catalytic hydrogenation, [77], solar cells, [78], advanced oxidation processes (AOPs), [79-81], and excellent performance efficiencies have been recorded. Only a few studies have been conducted on the technology of Cu and Ni-based bimetallic organic framework carbon materials, which have great potential in removing NPs in aqueous systems. Apart from that, Cu-C NCs and Ni-C NCs were reported for supercapacitor electrode application and electrocatalytic oxidation of phenol, respectively, [82, 83]. In the light of all this information, the development of non-noble Cu-Ni carbon materials (CuNi@C) that can effectively remove NPs from water; It is a new approach that is effective and important in preventing the pollution caused by NPs in the ecosystem.

Based on data given above inn this study, the maximum PET NPs removal efficiency was investigated under optimum conditions by using various experimental parameters to improve the efficiency using Ni-Cu-C NCs in an activated sludge solution. The effect of increasing pH values (4.0, 5.0, 6.0, 7.0 and 8.0), increasing adsorption times (30 min, 60 min, 90 min and 120 min), different Ni-Cu-C NCs adsorbent concentrations (100 mg/l, 200 mg/l, 300 mg/l and 400 mg/l) and different PET NPs concentrations (1 mg/l, 5 mg/l, 10 mg/l and 15 mg/l) in an activated sludge process on PET removal during adsorption process was investigated. The characteristics of the synthesized NCs were assessed using XRD, FTIR, FESEM, EDX and HRTEM analyses, respectively. In addition to, experimental results were evaluated with ANOVA statistical analysis.

2 Materials and Methods

2.1 Chemicals

As a pure powder activated carbon (PAC) source, powder activated charcoal was purchased from Sigma-Aldrich, German. Nickel (II) nitrate hexahydrate [$Ni(NO_3)_2.6H_2O$] (98%), copper (II) nitrate hexahydrate [$Cu(NO_3)_2.6H_2O$] (98%), sodium hydroxide [NaOH] (98%), potassium hydroxide [KOH] (99%) and hydrochloric acid [HCl] (37%) were provided from Sigma-Aldrich, Germany. PET (granular) was purchased from Sigma-Aldrich, Germany.

2.2 Synthesis of Ni-Cu-C NCs Adsorbents

Pure powder activated charcoal as a PAC were synthesized using a 2.2 N KOH solution and heated at 500°C for 5 h. The washed and dried 70 g PAC was soaked in 2.4 N/600 ml KOH overnight. The filtered blackish-wet carbonic solid was washed several times with 0.15 M HCl and with deionized water until obtaining a neutral pH=7.0 level of the wet carbonic solid. The dried and washed black-carbonic solid was then heated for 5 h at 500°C. The Ni-Cu-C NCs were prepared at increasing concentrations (100 mg/l, 200 mg/l, 300 mg/l and 400 mg/l) of Ni−Cu loaded on PAC. 2.2 g of PAC was dispersed in 85 ml of deionized water under ultrasonication for 25 min. An appropriate amount of $Cu(NO_3)_2.6H_2O$ and $Ni(NO_3)_2.6H_2O$ was dissolved separately in 25 ml of deionized water and then added to the PAC/H_2O suspension with stirring for 25 min. 2.2 M NaOH solution was added dropwise to the metal ions' PAC suspension until the pH level was 11.0, with stirring for 35 min, and then heated at 155°C in an autoclave for 3 h. The dried mass washed and filtered. Then, Ni-Cu-C NCs were separately calcined at 450°C for 5 h.

2.3 Activated Sludge Solution

Activated sludge was obtained from a municipal wastewater treatment plant in İzmir, Turkey. Activated sludge was used for experimental studies in the laboratory conditions.

2.4 Characterizations

2.4.1 X-Ray Diffraction (XRD) Analysis

Powder XRD patterns were recorded on a Shimadzu XRD-7000, Japan diffractometer using Cu Kα radiation (λ=1.5418 Å, 40 kV, 40 mA) at a scanning speed of 1^o min^{-1} in the 10-80^o 2θ range.

2.4.2 Raman Spectrum Analysis

Raman spectrum data was collected with a Horiba Jobin Yvon-Labram HR UV-Visible NIR (200-1600 nm) Raman microscope spectrometer, using a laser with λ=512 nm. The spectrum was collected from 10 scans at a resolution of 2 cm^{-1}. The zeta potential was measured with a SurPASS Electrokinetic Analyzer (Austria) with a clamping cell at 300 mbar.

2.4.3 Fourier Transform Infrared Spectroscopy (FTIR) Analysis

The FTIR spectra of samples was recorded using the FT-NIR spectroscope (RAYLEIGH, WQF-510). Experimental samples were scanned using infrared light and their chemical properties were observed in FTIR spectra.

2.4.4 Field Emission Scanning Electron Microscopy (FESEM) Analysis

The morphological features and structure of the synthesized catalyst were investigated by FESEM (FESEM, Hitachi S-4700). FESEM images were used to investigate the composition of the elements present in the synthesized nanocomposite.

2.4.5 Energy Dispersive X-Ray (EDX) Spectroscopy Analysis

The morphological features and structure of the synthesized catalyst were investigated by an EDX spectrometry device (TESCAN Co., Model III MIRA) to investigate the composition of the elements present in the synthesized catalyst.

2.4.6 High Resolution Transmission Electron Microscopy (HRTEM) Analysis

The structure of the samples was analyzed by HRTEM analysis. HRTEM analysis was recorded in a Technai G2 F20 S-TWIN TEM/HR(S)TEM (FEI, USA) under 200 kV accelerating voltage. Samples were prepared by applying one drop of the suspended material in ethanol onto a carbon-coated copper HRTEM grid and allowing them to dry at 25°C.

2.4.7 N_2 Adsorption Desorption and Pore Size Measurement

Adsorption and desorption isotherms were measured with nitrogen gas. Pore volume and pore area distributions were attained using the Barrett, Joyner, and Halenda (BJH) method and the reference curve of Harkins-Jura was used.

2.4.8 Raman Spectroscopy

Raman spectroscopy is based on Raman scattering, an inelastic scattering process that is only observed in a tiny proportion (~1 in 10^6) of the photons scattered by a molecule.

2.4.9 Measurement of CV Curves

Electrochemical experiments (CV) were performed on each electrode using the CHI 605E and DH-7000 electrochemical workstations for both the three-electrode system and the two-electrode system. The specific capacity for the nanocomposite system was calculated using Equation (1):

$$Q_m = \frac{I x \Delta t}{m} \quad (1)$$

In the equation: Q_m : is the specific capacity (C/g); I: is the charge/discharge current (A); Δt: is the discharge time (s) and m: is the mass of the active material (g).

2.5 Adsorption Mechanism

The adsorption mechanisms of NPs by chemically synthesized with larger sizes are based on hydrogen bonds, electrostatic between NPs and sponge materials are π-π interactions, [55, 59]. NPs in aquatic environments generally have a negative charge and can easily interact electrostatically with positively charged substances and be adsorbed on the surface. In comparison, the adsorption mechanisms of NPs via micromotors with smaller sizes are generally based on the phoretic interactions and shoveling, noncontact shoveling, and adsorptive bubble separation. Previous studies have reported that the synergetic adsorption mechanisms of surface and bubble separations also played a critical role in NPs adsorption, [59, 84-87]. The mechanisms of sorption of NPs removal during ASP in WWTPs was determined in Fig. 1.

* Fig. 1 can be found in the Appendix section.

The adsorption process forms a layer of adsorbate (metal ions) on the surface of adsorbents. Adsorption can be reproduced for multiple applications via a desorption method (reverse adsorption in which adsorbate ions are transported from the adsorbent surface) because adsorption is a reversible process in certain circumstances, [88]. Adsorption onto a solid adsorbent includes three major steps: transportation of the pollutant to the adsorbent surface from aqueous solution, adsorption onto the solid surface, and transport within the adsorbent particle. Generally, electrostatic attraction causes charged pollutants to adsorb on differently charged adsorbents because heavy metals have a vigorous affinity for hydroxyl (OH^-) or other functional group surfaces, [89].

The critical mechanisms of NPs removal during ASP are biodegradation or biotransformation and sorption. The main mechanisms of NPs biodegradation include sequential steps of assimilation and mineralization, [90]. The NPs get incorporated or ingested by microorganisms like metazoan or protozoan and subsequently get hydrolysed into simpler units via intracellular degradation, [91]. Also, the NPs can be degraded into simpler units by hydrolases like extracellular enzymes secreted by microorganisms via extracellular degradation, [61]. The simpler units, further metabolized by the various metabolic pathways and final end products like CO_2, H_2O, CH_4, are produced via the process of mineralization. Different biodegradation mechanisms can be observed based on the chemical structure and polymer types of the NPs, [92]. Different enzymes like protease, laccase, esterases, cutinase, etc., have exhibited encouraging results in the NPs degradation, [90, 93].

2.6 Adsorption Isotherm

Adsorption isotherms play a vital role in interpreting the mechanism of metal ion adsorption onto different adsorbents, [94]. Adsorption kinetic models shed light on the surface properties of adsorbents and the intermolecular interactions between adsorbed molecules and the adsorbent matrix, [95]. Isotherm and kinetic models contribute to understanding the adsorption process, relying on various factors, including the adsorbent's structure and the physical and chemical characteristics of the solute, [94]. The Langmuir model finds application in solid–liquid systems, elucidating that all sites on the surface of the adsorbent have equal opportunities to be occupied by heavy metals (such as Cu, Ni) in Equation (2):

$$q_e = \frac{q_{max} K_L C_e}{1 + K_L C_e} \quad (2)$$

where; q_e: amount of adsorbed metal ions per unit mass of adsorbent at equilibrium (mg/g), C_e: metal ion concentration in solution at equilibrium (mg/l), K_L: Langmuir binding constant (l/mg), q_{max}: maximum amount of metal adsorbed per unit weight of adsorbent (mg/g).

The main properties of Langmuir model adsorption isotherms for Ni-Cu-C NCs were determined to homogeneous surface of bio-adsorbents, mono layer adsorption, adsorbate amount has no influence on the adsorption kinetic, no interaction between the adsorbed molecules and a dimensionless model.

Note that the best-fit R^2 values calculated from both the Langmuir model (0.995-0.999) and the Freundlich model (0.983-0.997) are relatively close to 1, indicating that both models can accurately describe the adsorption process at different temperatures (i.e., 20ºC, 30ºC and 40ºC). However, R^2 values obtained from the Langmuir model were slightly greater than those from the Freundlich model for both the unary and the binary adsorptive systems, suggesting that the former model is better in defining these adsorption isotherm data and that both heavy metal ions were likely to occur in a monolayer manner based on the basic assumption of the Langmuir model [96].

2.7 Adsorption Kinetic

Kinetic adsorption models describe the mechanism of adsorption of Ni-Cu-C NC by biosorbents and particularly determine the rate of biosorption during the removal of heavy metals from wastewater on an industrial scale to optimize the design parameters, including the adsorbate residence time and reactor dimension, [95]. Heavy metals (Cu, Ni) kinetics; It conforms to the pseudo-second order adsorption kinetics (non-linear form) in Equation (3):

$$q_t = \frac{k_2 q_e^2 t}{1 + k_2 q_e^2 t} \quad (3)$$

where; q_e (mg/g): adsorption capacity at equilibrium, q_t (mg/g): adsorption capacity at time t (min), k_2 (g/mg.min): pseudo-second-order rate constant, respectively.

The main properties of pseudo-second order adsorption kinetics of heavy metals were summarized to the second-order rate equation, detected as the best suitable model with highest R^2 value, express chemical adsorption of ions, which involve valence forces, chemical coordination through sharing or exchange electrons between adsorbent and heavy metals (ion exchange), the rate of occupation of adsorption sites is proportional to the square of the number of unoccupied sites.

2.8 Statistical Analysis

ANOVA analysis of variance between experimental data was performed to detect F and *P* values. The ANOVA test was used to test the differences between dependent and independent groups, [97]. Comparison between the actual variation of the experimental data averages and standard deviation is expressed in terms of F ratio. F is equal (found variation of the date averages/expected variation of the date averages). *P* reports the significance level, and d.f indicates the number of degrees of freedom.

Regression analysis was applied to the experimental data in order to determine the regression coefficient R^2, [98]. The aforementioned test was performed using Microsoft Excel Program.

All experiments were carried out three times and the results are given as the means of triplicate samplings. The data relevant to the individual pollutant parameters are given as the mean with standard deviation (SD) values.

3 Results and Discussions

3.1 XRD Analysis Results

The results of XRD analysis observed for Ni-Cu-C NCs in an activated sludge solution with adsorption process for PET NPs removal is illustrated in Fig. 2. The characterization peaks were measured at 2θ values of 24.70°, 35.65°, 38.11° and 43.82°, respectively, corresponding to the (100), (120), (302) and (002) planes of implying Ni-Cu-C NCs (red spectrum) in an activated sludge solution for PET NPs removal via adsorption after 30 min adsorption time (Fig. 2a). The characterization peaks were obtained at 2θ values of 25.08°, 36.22°, 37.75°, 42.31°, 47.16°, 57.24°, 64.11° and 66.33°, respectively, corresponding to the (010), (110), (111), (021), (121), (211), (220) and (311) plans, respectively, implying Ni-Cu-C NCs (green spectrum) in an activated sludge solution for PET NPs removal after 60 min adsorption time (Fig. 2b). The characterization peaks were found at 2θ values of 24.27°, 32.36°, 38.11°, 39.42°, 42.10°, 47.25°, 58.34°, 65.28° and 67.34°, respectively, corresponding to (100), (011), (110), (111), (021), (200), (121), (202) and (032), respectively, implying Ni-Cu-C NCs (blue spectrum) in an activated sludge solution for PET NPs removal after 90 min adsorption time (Fig. 2c). The characterization peaks were observed at 2θ values of 24.29°, 35.17°, 38.83°, 39.21°, 42.33°, 47.20°, 58.24°, 64.60°, and 67.78°, respectively, corresponding to (002), (111), (021), (121), (202), (033), (210), (302), and (104) respectively, implying Ni-Cu-C NCs (pink spectrum) in an activated sludge solution for PET NPs removal after 120 min adsorption time (Fig. 2d).

* Fig. 2 can be found in the Appendix section.

Note the detailed XRD spectrum of similar Ni-Cu samples was reported previously [99]. Based on XRD data, the adsorption process of the Ni-Cu-C NCs premix for 3 min does not result in the alloy formation. It is represented by a mixture of metals. The formation of an alloy occurs during the heating of this sample in an inert atmosphere to the reaction temperature (at 25°C).

3.2 FTIR Analysis Results

The FTIR spectrum of Ni-Cu-C NCs were determined in an activated sludge solution during PET NPs removal via adsorption (Fig. 3). The main peaks of FTIR spectrum for Ni-Cu-C NCs (red spectrum) was observed at 542 cm^{-1}, 706 cm^{-1}, 1005 cm^{-1}, 1478 cm^{-1}, 1758 cm^{-1} and 3751 cm^{-1} wavenumber, respectively, after 30 min adsorption time during PET removal (Fig. 3a). The main peaks of FTIR spectrum for Ni-Cu-C NCs (green spectrum) was obtained at 618 cm^{-1}, 645 cm^{-1}, 1010 cm^{-1}, 1434 cm^{-1}, 1751 cm^{-1} and 3758 cm^{-1} wavenumber, respectively, after 60 min adsorption time during PET NPs removal (Fig. 3b). The main peaks of FTIR spectrum for Ni-Cu-C NCs (blue spectrum) was determined at 551 cm^{-1}, 744 cm^{-1}, 1018 cm^{-1}, 1539 cm^{-1}, 1701 cm^{-1} and 3715 cm^{-1} wavenumbers, respectively, after 90 min adsorption time for PET NPs removal (Fig. 3c). The main peaks of FTIR spectrum for Ni-Cu-C NCs (pink spectrum) was obtained at 516 cm^{-1}, 638 cm^{-1}, 1074 cm^{-1}, 1479 cm^{-1}, 1724 cm^{-1} and 3729 cm^{-1} wavenumber, respectively, after 120 min adsorption time during PET NPs removal (Fig. 3d).

* Fig. 3 can be found in the Appendix section.

Minteniget al., [100], used FPA-based transmission micro-FTIR to identify NPs in wastewater and sludge samples, limiting fibre size (10–20 lm) and lateral resolution. Xu et al., [101], collected 68 influent and 72 effluent samples from WWTPs and found 112 plastics of 14 different types, which includes polyethylene (PE), polyamide (PA), polypropylene (PP), polystyr ene (PS), PET, rayon, polyvinyl chloride (PVC), poly methylmethacrylate (PMMA), rubber, polyethylene and polyether urethane (PU), polypropylene copolymer (PE-PP), acrylonitrile styrene copolymer (AS) and poly acrylate (PA).

3.3 FESEM Analysis Results

The morphological features of Ni-Cu-C NCs were characterized through FESEM images (Fig. 4). The FESEM images of Ni-Cu-C NCs were obtained in an activated sludge solution with adsorption process for PET NPs removal (Fig. 4).

* Fig. 4 can be found in the Appendix section.

As is seen, the material is represented by rather short carbon filaments (nanofibers) grown on the

particles of the Ni-Cu alloy (Fig. 4). It is worth noting that the formed active metal particles are mainly of biconical shape (Fig. 4). The carbon filaments grow predominantly in two opposite directions. As follows from the microscopic data, 1 min of exposure to the reaction mixture is enough for the almost complete destruction of the bulk alloy and the formation of active particles catalyzing the growth of carbon naofibers (Fig. 4).

Similar tangles of thin carbon nanofibers were obtained previously when decomposing the mixture of C2–C4 hydrocarbons on the Ni-Cr alloy [102]. The composite material is represented by carbon filaments with catalytic particles embedded in their structure. Such carbon composite materials with embedded metal particles were reported to exhibit high catalytic activity in electrocatalytic reactions [103].

3.4 EDX Analysis Results

The EDX analysis was also performed to investigate the composition of Ni-Cu-C NCs (Fig. 5). The EDX analysis exhibited the composition of Ni-Cu-C NCs in an activated sludge during adsorption process for PET NPs removal after 120 min adsorption time (Fig. 5).

* Fig. 5 can be found in the Appendix section.

According to EDX analysis Ni and Cu atoms are predominantly found in the active particles. EDX data it also suggests that the formation of Ni-Cu-C NCs particles does not occur during spontaneous events due to redistribution of Ni and Cu atoms.

In addition to the EDX mapping, the Ni and Cu atoms are predominantly located in the same areas related to the active particles. The EDX data also suggest that no redistribution of the Ni and Cu atoms occurs during the spontaneous formation of catalytic particles.

3.5 HRTEM Analysis Results

The HRTEM images of Ni-Cu-C NCs exhibited a micromorphological structure in the activated sludge solution process during PET NPs removal after 120 min adsorption time (Fig. 6).

* Fig. 6 can be found in the Appendix section.

Since the Ni-CuC alloy was formed during the heating of the Ni-Cu-C sample to the reaction temperature, the elemental composition of the obtained particles was analyzed in detail by HRTEM (Fig. 6). Therefore, the high-resolution HRTEM images of the filament suggest that the carbon layers are quite tightly stacked together.

3.6 Nitrogen Adsorption/Desorption Study Analysis

Nitrogen adsorption/desorption curves and the corresponding Barrett-Joyner-Halenda (BJH) pore diameter distribution diagram is used to analyze the samples of Ni-Cu-C NCs in Fig. 7a shows that the curves of the aforementioned nanocomposite are all of type-iv isotherms and have obvious hysteresis loops, indicating abundant pore structures. More details on the porosity of material were obtained by BET and BJH analyses, as shown in Fig. 7b.

* Fig. 7 can be found in the Appendix section.

The specific surface area of Ni-Cu-C and Cu-C N Cs are 27.3 m^2/g and 12.1 m^2/g, respectively. However, the specific surface area of Ni-Cu-C NC is 52.7 m^2/g. The 3D skeleton of porous nanosheets composed of many nanoparticles provides a larger specific surface area as analyzed in Fig. 7(a-d). In addition, the pore sizes of Ni-Cu-C NC is concentrated at 4 nm, respectively, while Cu-C and Ni-Cu NCs show a smaller and richer pore size distribution at 2 nm. It is conducive to the infiltration of electrolyte ions, so as to obtain more reaction sites, which is conducive to the rapid transfer of charge, and improve the specific adsorption capacity of nanocomposite.

3.7 Raman Spectroscopy

To further check the graphitic character of the composites, the materials were characterized by Raman spectroscopy. The Raman spectra were recorded in the range of 100–3500 cm^{-1}, which is the most informative for carbon materials (Fig. 8). Raman spectroscopy is a non-destructive and powerful technique used to identify and characterize all the members of the carbon family. Raman spectra measured at the lowest laser powers of 0.1÷1mW are dominated by one-phonon peaks attributed to the G-(~1590 cm^{-1}) and D-bands (~1350cm^{-1}) of disordered sp2 carbon. Less intense second-order peaks are attributed to 2D (~2710 cm^{-1}), D+G (~2940 cm^{-1}) and 2G (~3200 cm^{-1}) bands.

* Fig. 8 can be found in the Appendix section.

In detail, the G-band refers to sp2 carbon atoms scattering due to vibrations of the E2g mode, while the D-band represents internal defect-induced scattering. The shape of the Raman spectra indicates crystallization of graphitic structures with a low

graphitization degree typical for nanographite as evidenced both by the rather high full-width of the G-band and the ID/IG ratio (data not shown). The ID/IG intensity ratio gives a measure of the structural disorder and makes it possible to estimate the average in-plane crystallite size (La) of the sp2 domains according to the relation I I D G / 0 = .0055La 245.46. The Cu/C nanocomposite shows the most disordered nanographite phase as evidenced by having both the highest full width of the G and D bands and the lowest estimated crystallite size La. Therefore, Raman analysis demonstrated that nickel, in comparison to cobalt and copper, promotes the formation of a more ordered sp2 carbon structure. Enhanced formation of the more ordered nanographite phase leading to a higher thickness of carbon shell around the metal nanoparticles, therefore, appears to be the reason for the increased carbon content in the composites obtained particularly using Co and Ni.

3.8 CV Curves of Ni-Cu-C NCs

The CV curves of all samples and pure nickel foam (NF) at scanning rates of 5 mV/s are compared in Fig 9. They all showed obvious redox peaks, which are caused by Ni^{2+}/N^{3+}, Co^{2+}/Co^{3+} and Cu^{2+}/Cu^{+} electron pairs in the redox reactions. It can be clearly seen that the CV curve of Ni-Cu-C NCs covers a higher area than Ni-Cu and Ni-C NCs which means that Ni-Cu-C NCs has a higher energy storage capacity. It is due to the large specific surface area of Ni-Cu-C NCs, which can increase the number of reactive sites and thus improve the specific capacity.

* Fig. 9 can be found in the Appendix section.

To investigate the charge/discharge mechanism of the electrode, the relationship between anodic peak current and the square root of scan rate of different samples. The correlation coefficients obtained after linear fitting are all greater than 0.99, indicating that there is a linear relationship between the anodic peak current and the square root of the scanning rate, that is, the electrochemical energy storage kinetics is mainly controlled by the diffusion of OH^- (data not shown). Moreover, it is obvious that the slope of the fitting line of Ni-Cu-C NCs is the larger, indicating that the two have higher diffusion rates. Furthermore, the relationship between the current and the scan rates of each redox peak of Ni-Cu-C NCs/ Ni-Cu NCs is calculated by the following formula in Eq. (4):

$$i = av^b \quad (4)$$

where; i (A): is the current, v: is the scanning rate (mV/s). The b: is the slope value of the curve between the logarithmic peak current and the logarithmic scanning rate. The value of b ranges from 0.5 to 1.0. When the value of b is close to 1, the electrochemical reaction of the nanocomposite is capacitive behavior, while when the value of b is close to 0.5, the reaction is battery behavior, which is controlled by ion diffusion. The values of b of the redox peaks of Ni-Cu-C NCs/Ni-Cu NCs are 0.87 and 0.84 respectively, both within the range of 0.5–1.0. It shows that the reaction process of nanocomposite is controlled by capacitor behavior and battery behavior simultaneously.

3.9 Effect of Some Operational and Environmental Conditions on PET NPs Yields

3.9.1 Effect of pH Values

The impacts of increasing pH values (4.0, 5.0, 6.0, 7.0 and 8.0) on removals of PET NPs were examined in an activated sludge solution during adsorption process at 25ºC (Fig. 10). 43.21%, 68.93%, 75.11%, 99.31% and 40.09% PET NPs removals were measured at pH=4.0, at pH=5.0, at pH=6.0, at pH=7.0 and at pH=8.0, respectively, in an activated sludge solution during adsorption process, at 25ºC (Fig. 10). The maximum 99.31% PET NPs removal was obtained at pH=7.0 in an activated sludge solution during adsorption process, at 25ºC (Fig. 10).

* Fig. 10 can be found in the Appendix section.

In adsorption studies, pH of solution plays pivotal role in the electrostatic interactions between adsorbates and adsorbents. In basic conditions, formation precipitation of metal ions as their respective hydroxide can infuence the adsorption results, therefore we have selected the maximum adsorption under acidic environment. As pH increases the surface of NPs become more negatively charged. This causes increased repulsion between PET and Ni-Cu-C NCs. Hence the removal efficiency decreases with increase in pH. Also change in PET uptake with pH is shown graphically. The ANOVA test indicated no significant differences between pH value and NPs yields up to a pH value of pH=7.0 ($p = 0.06$, $F = 0.25$, d.f. = 2). The ANOVA test indicated significant differences between pH values and NPs yields for adsorption times > pH=7.0 and < 5.0 ($p = 0.74$, $F = 3.21$, d.f. = 2).

The pH value can change the zeta potential of NPs or heavy metal precipitation, thereby increasing or decreasing the adsorption of certain metals. Generally, pH value increases with the decreasing zeta potential of NPs. However, if the NP's zero-

charge point is below the pH of the water, the NP charge will be negative. Thus, the electrostatic attraction between the metals and the polymer increases. In contrast, precipitation of some metals may occur in environments with a pH around 7.0. A recent study reported that pH increases with increasing the adsorption of Cu, zinc (Zn), Ni, cadmium (Cd), lead (Pb), and cobalt (Co) by NPs [104, 105-111].

3.9.2 Effect of Adsorption Time

Effects of increasing adsorption times (30 min, 60 min, 90 min and 120 mins on PET NPs removals in an activated sludge solution during adsorption process at pH=7.0 and at 25^{o}C is illustrated in Fig. 11. 38.54%, 61.73%, 86.29% and 99.42% PET NPs removals were measured after 30 min, 60 min, 90 min and 120 min adsorption time, respectively, in an activated sludge process during adsorption process, at pH=7.0 and at 25^{o}C (Fig. 11). The maximum 99.42% PET NPs removal was observed after 120 min adsorption time, in an activated sludge solution during adsorption process, at pH=7.0 and at 25^{o}C (Fig. 11).

* Fig. 11 can be found in the Appendix section.

As time progresses the surface coverage of the adsorbent is high an adsorption process takes place. Increasing the contact time between the PET and Ni-Cu-C NCs adsorbent would improve the percentage removal. Increases in time are expected to enhance sorption until saturation at equilibrium. The ANOVA test indicated no significant differences between time and NPs yields up to a adsorption time of 120 min ($p = 0.04$, $F = 0.22$, d.f. = 2). The ANOVA test indicated significant differences between adsorption times and NPs yields for adsorption times > 120 min ($p = 0.47$, $F = 3.18$, d.f. = 2).

3.9.3 Effect of Ni-Cu-C NCs Adsorbent

The impact of increasing Ni-Cu-C NCs adsorbent concentrations (100 mg/l, 200 mg/l, 300 mg/l and 400 mg/l) on PET NPs removals in an activated sludge process during adsorption process was investigated after 120 min adsorption time, at pH=5.0 and at 25^{o}C (Fig. 12). 39.50%, 70.05%, 99.20% and 86.43% PET NPs removals were observed at 100 mg/l, 200 mg/l, 300 mg/l and 400 mg/l Ni-Cu-C NCs adsorbent concentrations, respectively, in an activated sludge solution during adsorption process, after 120 min adsorption time, at pH=7.0 and at 25^{o}C (Fig. 12). The maximum PET NPs removal was obtained as 99.20% for 300 mg/l Ni-Cu-C NCs adsorbent concentration, in an activated sludge solution during adsorption process, after 120 min adsorption time, at pH=7.0 and at 25^{o}C (Fig. 12).

* Fig. 12 can be found in the Appendix section.

This may be due to overlapping of the adsorption sites as a result of overcrowding of the adsorbent particles. It is seen that percent removal increases with the increase in the concentration of the adsorbent. The maximum percent removal is exhibited at a adsorbent concentration of 300 mg/l. This is due to enhanced active sites with an optimum increase in amount of adsorbent. As can be observed in over trend of adsorption with the adsorbent dosage, the adsorption increases with the increase in dosage and reached to maximum value at 300 mg/l. These, observations suggest that adsorption is almost directly proportional to the amount of the dosage. The ANOVA test indicated no significant differences between Ni-Cu-C NCs adsorbent concentration and NPs yields up to an adsorbent concentration of 300 mg/l ($p = 0.05$, $F = 0.34$, d.f. = 2). The ANOVA test indicated significant differences between adsorbent concentrations and NPs yields for adsorpbent concentrations > 300 mg/l ($p = 0.51$, $F = 3.06$, d.f. = 2).

3.9.4 Effect of PET NPs Concentration

The impact of increasing PET NPs concentrations (1 mg/l, 5 mg/l, 10 mg/l and 15 mg/l) on the adsorption of PET NPs were investigated in an activated sludge solution in the present of 300 mg/l Ni-Cu-C NCs adsorbent concentration, after 120 min adsorption time, at pH=7.0 and at 25^{o}C (Fig. 13). 37.83%, 74.26%, 99.31% and 88.02% PET NPs removals were observed to 1 mg/l, 5 mg/l, 10 mg/l and 15 mg/l PET NPs concentrations, respectively, in an activated sludge solution during adsorption process, with 300 mg/l Ni-Cu-C NCs adsorbent concentration, after 120 min adsorption time, at pH=5.0 and at 25^{o}C (Fig. 13). The maximum 99.31% PET NPs removal was measured for 10 mg/l PET NPs concentration (Fig. 13).

* Fig. 13 can be found in the Appendix section.

When more adsorbate molecules bind to the active sites of the adsorbent, diffusion accelerates the binding of PET on the surface of the Ni-Cu-C NCs due to the increase in driving force of concentration gradient, resulting in higher adsorption capacities. However, a decline of adsorption efficiency due to higher pollutant concentration. At higher pollutant concentrations, the number of available adsorbent sites becomes fewer, resulting in a decrease in

pollutant removal efficiency. The ANOVA test indicated no significant differences between PET NPs concentration and NPs yields up to a PET NPs concentration of 10 mg/l ($p = 0.07$, $F = 0.20$, d.f. = 2). The ANOVA test indicated significant differences between PET NPs concentrations and NPs yields for PET NPs concentrations > 10 mg/l ($p = 0.61$, $F = 3.02$, d.f. = 2).

3.10 Optimization of the Experimental Conditions in an Aerobic Activated Sludge Treatment Plant

In this study, the high concentrations of PET NPs were not treated effectively in a continuous flow activated sludge process. Before aerobic activated sludge process the biomass concentration returned by the aeration tank was mixed with 1 liter wastewater containing 10 mg/l PET NP concentration and 300 mg Ni-Cu-C NCs during 120 min adsorption time, at pH=7.0 and at 25^{o}C. After this duration the PET NPs was removed with yields as high as around 99.20% and 99.42%. No pH adjustement was performed for activated sludge and during PET removal since the pH of wastewater was 7.0.This decreased the cost of the treatment. After this step with specific gravity and settling ability and focculation of sludge focs with nanocomposite the treated water was separated from the wastewater. The COD and BOD removals were improved in the next activated sludge process because of the adsorption of non-biodegradable and slowly biodegradable PET NP materials. The Ni-Cu-C NCs nanocomposite was reused and used again in the continuous removal of PET from wastewater. Therefore, this process is environmentally friendly and cost-effective, as it realizes the recycling of an industrial waste. These experimental fndings demonstrated a novel, reliable and efective technology for the utilization of Ni-Cu-C NCs. Tis process concept can be further applied in the full scale aerobic biological treatment systems and generally in municipal and industrial wastewater treatment facilities.

4 Conclusion

NPs cause more serious environmental problems than plastics and microplastics. Due to the difficult degradation processes of NPs, difficulties in recycling rates, large specific surface areas, and ability to transform into more complex and toxic structures by adsorbing other pollutants, they can easily enter the food chain and other environments. To ensure effective adsorption of NPs in the aquatic environment; many studies have been conducted on the enrichment and removal of NPs in the aquatic environment, such as the preparation of adsorption materials using various natural products of animals and plants, and various studies on this subject are continuing.

Adsorption is widely used for the removal of contaminants from aqueous solutions, being cost-effective and environmentally friendly treatment process. The possible factors affecting the removal efficiency of NPs by adsorption process include: pH, adsorbent concentrations, adsorption time, temperature and NP concentrations.

In this study, the maximum PET NPs removal efficiency was investigated under optimum conditions by using various experimental parameters (pH, adsorption time, adsorbent concentrations and NPs concentrations) to improve the efficiency of PET adsorption yields using Ni-Cu-C NCs from an activated sludge solution. The maximum 99.20-99.42% PET NPs removal was measured at 10 mg/l PET NPs concentration, in an activated sludge process during adsorption process, at 300 mg/l Ni-Cu-C NCs adsorbent concentration, after 120 min adsorption time, at pH=7.0 and at 25^{o}C. The adsorption process was found to be a very effective method in the removal of PET NPs from an activated sludge solution with Ni-Cu-C NCs adsorbent. Adsorption process; is an easily applicable, environmentally friendly and economical method.

The Langmuir model finds application in solid–liquid systems, elucidating that all sites on the surface of the adsorbent have equal opportunities to be occupied by heavy metals (such as Cu, Ni). Heavy metals (Cu, Ni) kinetics; It conforms to the pseudo-second order adsorption kinetics (non-linear form).

Based on XRD data, the adsorption process of the Ni-Cu-C NCs premix for 3 min does not result in the alloy formation. It is represented by a mixture of metals. The formation of an alloy occurs during the heating of this sample in an inert atmosphere to the reaction temperature at 25^{o}C. FTIR spectrum is the most commonly used technique for detecting NPs. It exposes plastic particles to infrared radiation, producing spectra that correspond to the vibrations of chemical bonds between different atoms. The FTIR spectra were then compared with the reference spectra stored in a library to analyze the composition of the NPs. According to, FESEM and HRTEM analyses, during the carbon erosion process, the initial microdispersed Ni-Cu alloy disintegrates on small metal particles, which catalyzes the growth of carbon nanofibers. EDX mapping confirmed that the distribution of metal atoms in these particles is uniform and corresponds to the Ni/Cu weight ratio of

Ni/Cu=88/12, which was specified during the synthesis.

In WWTPs, the elimination of NPs is of great importance in every aspect, as the key point connecting urban and social water use.

One of the aspects of NPs pollution is their carrying and transfer from one environment to another, increasing general contamination and the risk of ecotoxicity. To reduce NPs emissions in the environment, it is very important and necessary to adopt "sustainable plastic waste management" practices, as well as to improve technologies and processes for their removal from WWTPs. NPs control and reduce their sources should be performed bu using "comprehensive monitoring programs".

Most advanced purification technologies for NPs removal are implemented at laboratory scales; For practical applications, full-scale application feasibility must be investigated and its applicability must be ensured. In order to evaluate the contribution of WWTPs to NP pollution; There is a great need for more detailed research and evaluation of the available data to understand the degradation mechanism of NPs in aquatic environments.

Different international organizations and governments around the world should urgently make the necessary plans to create implementation frameworks to reduce or prevent plastic pollution in the environment by raising public awareness about plastic pollution, switching to biodegradable products, and discouraging the production and consumption of plastics, and put these plans into practice immediately. They must take the necessary steps to an important future perspective is to better recycle and reuse plastics; Optimizing waste management systems and evaluating the life cycle of NPs are also very important, and their implementation is very necessary.

Finaly, plastics are one of the most important materials for almost all areas of work. Plastics are important that their correct use and, as far as possible, their reduction, added to the good management of waste to avoid the dangers that plastic can mean and in our lives.

Acknowledgement:
Experimental analyzes in this study were performed at the Laboratories of the Canada Research Center, Ottawa, Canada. The authors would like to thank this body for providing financial support.

References:

[1] R. Geyer, J.R. Jambeck, K.L. Law, Production, Use, and Fate of All Plastics Ever Made, *Science Advances*, Vol.3, No.7, 2017, pp. 1-5, e1700782.

[2] S.S. Ali, T. Elsamahy, R. Al-Tohamy, D. Zhu, Y. A.-G. Mahmoud, E. Koutra, M.A. Metwally, M. Kornaros, J. Sun, Plastic Wastes Biodegradation: Mechanisms, Challenges and Future Prospects, *Science of the Total Environment*, Vol.780, 2021, 166590.

[3] H. Andrade, J. Glüge, D. Herzke, N.M. Ashta, S.M. Nayagar, M. Scheringer, Oceanic Long-Range Transport of Organic Additives Presents in Plastic Products: An Overview, *Environmental Sciences Europe*, Vol.33, No.1, 2021, Article number: 85.

[4] R. Barra, S.A. Leonard, *Plastics and the Circular Economy*, in: 54th Global Environment Facility Council Meeting, Da Nang, Vietnam, June 24-26, 2018. GEF/STAP/C.54/Inf.05.

[5] J.M. Garcia, M.L. Robertson, The Future of Plastics Recycling: Chemical Advances are Increasing the Proportion of Polymer Waste That Can be Recycled, *Science,* Vol.358, No.6365, 2017, pp. 870-872.

[6] B.H. Zainudin, T.W. Wong, H. Hamdan, Chapter 8: Pectin as Oral Colon-Specific Nano- and Microparticulate Drug Carriers, *Polymer Science and Innovative Applications: Materials, Techniques, and Future Developments*, 2020, pp. 257-286.

[7] O.S. Alimi, J. Farner Budarz, L.M. Hernandez, N. Tufenkji, Microplastic and Nanoplastic in Aquatic Environments: Aggregation, Deposition, and Enhanced Contaminant Transport, *Science of the Total Environment*, Vol.52, 2018, pp. 1704-1724, 2018.

[8] Y. Zhang, H. Jiang, K. Bian, H. Wang, C. Wang, A Critical Review of Control and Removal Strategies for Microplastics from Aquatic Environments, *Journal of Environmental Chemical Engineering*, Vol.9, No.4, 2021, 105463, 2021.

[9] R.Z. Habib, T. Thiemann, R. Al Kendi, Microplastics and Wastewater Treatment Plants a Review, *Journal of Water Resource and Protection*, Vol.12, No.01, 2020, pp. 1-35, 2020.

[10] P.R. Rout, M. Goel, A. Mohanty, D. S. Pandey, N. Halder, S. Mukherjee, S.K. Bhatia, N.K. Sahoo, S. Varjani, Recent Advancements in Microalgal Mediated Valorisation of Wastewater from Hydrothermal Liquefaction of Biomass, *BioEnergy Research*, Vol.16, 2022, pp. 45-60, 2022.

[11] J. Talvitie, A. Mikola, O. Setala, M. Heinonen, A. Koistinen, How Well is Microlitter Purified from Wastewater? – A Detailed Study on the Stepwise Removal of Microlitter in a Tertiary Level Wastewater Treatment Plant, *Water Research*, Vol.109, 2017, pp. 164–172.

[12] J. Talvitie, A. Mikola, A. Koistinen, O. Setälä, Solutions to Microplastic Pollution: Removal of Microplastics from Wastewater Effluent with Advanced Wastewater Treatment Technologies, *Water Research*, Vol.123, 2017, pp. 401–407.

[13] A.L. Andrady, M.A. Neal, Applications and Societal Benefits of Plastics, *Philosophical Transactions of the Royal Society of London. Series B, Biological Sciences*, Vol.364, 2009, pp. 1977–1984.

[14] R. Öztekin, D.T. Sponza, Removal Mechanisms of Polyethylene, Polypropylene, Polyvinyl Chloride, Polyamide (Nylon), Polystyrene and Polyethylene Terephthalate in Wastewater Treatment Plants by Chemical, Photocatalytic, Biodegradation and Hybrid Processes, *WSEAS International Journal of Environmental Engineering and Development*, Vol.1, 2023, pp. 206-238.

[15] F. Murphy, C. Ewins, F. Carbonnier, B. Quinn, Wastewater Treatment Works (WWTW) as a Source of Microplastics in the Aquatic Environment, *Environmental Science & Technology*, Vol.50, No.11, 2016, pp. 5800–5808.

[16] A. Rahimi, J. M. García, Chemical Recycling of Waste Plastics for New Materials Production, *Nature Reviews Chemistry*, Vol.1, No.6, 2017, Article number: 0046, pp. 1-11.

[17] R. Öztekin, D.T. Sponza, H_2 Production from Real Wastes of Polyethylene Terephthalate and Polylactic Acid Using CN_x/Ni_2P Nanocatalyst, *International Journal of Clinical Case Reports and Reviews*, Vol.14, No.4, 2023, pp. 1-15.

[18] I.A. Ignatyev, W. Thielemans, B. Vander Beke, Recycling of Polymers: A Review, *ChemSuschem*, Vol.7, No.6, 2014, pp. 1579-1593.

[19] L.D. Ellis, N.A. Rorrer, K.P. Sullivan, M. Otto, J. McGeehan, Y. Román-Leshkov, N. Wierckx, G.T. Beckham, Chemical and Biological Catalysis for Plastics Deconstruction, Recycling, and Upcycling, *Nature Catalysis*, Vol.4, No.7, 2021, pp. 539-556.

[20] I.H.S. Markit, *PET Polymer: Chemical Economics Handbook; 2021*, 2021. Access online on 15 September, 2024 at https://ihsmarkit. com/products/pet-polymer-chemical-economics -handbook.html.

[21] F. Awaja, D. Pavel, Recycling of PET, *European Polymer Journal*, Vol.41, No.7, 2005, pp. 1453-1477.

[22] A.B. Raheem, Z.Z. Noor, A. Hassan, M.K. Abd Hamid, S.A. Samsudin, A.H. Sabeen, Current Developments in Chemical Recycling of Post-Consumer Polyethylene Terephthalate Wastes for New Materials Production: A Review, *Journal of Cleaner Production*, Vol.225, 2019, pp. 1052-1064.

[23] S. Anupama, N. Luckins, R. Menon, S. Robert, T.S. Kumbalaparambi, Micro-plastics in the Vicinity of an Urban Solid Waste Management Facility in India: Assessment and Policy Implications, *Bulletin of Environmental Contamination and Toxicology*, Vol.109, No.6, 2022, pp. 956-961.

[24] M.C. Collivignarelli, S. Todeschini, S. Bellazzi, M. Carnevale Miino, F.M. Caccamo, S. Calatroni, M. Baldi, S. Manenti, Understanding the Influence of Diverse Non-Volatile Media on Rheological Properties of Thermophilic Biological Sludge and Evaluation of its Thixotropic Behaviour, *Applied Sciences*, Vol.12, No.10, 2022, 5198.

[25] M.C. Collivignarelli, F.M. Caccamo, S. Bellazzi, A. Abbà, G. Bertanza, Assessment of the Impact of a New Industrial Discharge on an Urban Wastewater Treatment Plant: Proposal for an Experimental Protocol, *Environments*, Vol.10, No.7, 2023, 108.

[26] M. Lapointe, J.M. Farner, L.M. Hernandez, N. Tufenkji, Understanding and Improving Microplastics Removal During Water Treatment: Impact of Coagulation and Flocculation, *Environmental Science and Technology*, Vol.54, 2020, pp. 8719–8727.

[27] H.S. Auta, C.U. Emenike, B. Jayanthi, S.H. Fauziah, Growth Kinetics and Biodeterioration of Polypropylene Microplastics by Bacillus Sp and Rhodococcus Sp Isolated from Mangrove Sediment, *Marine Pollution Bulletin*, Vol.127, 2018, pp. 15–21.

[28] J. Talvitie, A. Mikola, A. Koistinen, O. Setala, Solutions to Microplastic Pollution - Removal of Microplastics from Wastewater Effluent with Advanced Wastewater Treatment Technologies, *Water Research*, Vol.123, 2017, pp. 401–407.

[29] V.P. Kelkar, C.B. Rolsky, A. Pant, M.D. Green, S. Tongay, R.U. Halden, Chemical and Physical Changes of Microplastics during Sterilization by Chlorination, Water Research, Vol.163, 2019, 114871.

[30] L. Cai, J. Wang, J. Peng, Z. Wu, X. Tan, Observation of the Degradation of Three Types

of Plastic Pellets Exposed to UV Irradiation in Three Different Environments, Science of the Total Environment, Vol.628-629, 2018, pp. 740–747.

[31] B. Ma, W. Xue, C. Hu, H. Liu, J. Qu, L. Li, Characteristics of Microplastic Removal Via Coagulation and Ultrafiltration During Drinking Water Treatment, Chemical Engineering Journal, Vol.359, 2019, pp. 159–167.

[32] C. Sun, Z. Wang, L. Chen, F. Li, Fabrication of Robust and Compressive Chitin and Graphene Oxide Sponges for Removal of Microplastics with Different Functional Groups, *Chemical Engineering Journal*, Vol.393, 2020, 124796.

[33] P. Risch, C. Adlhart, A Chitosan Nanofiber Sponge for Oyster-Inspired Filtration of Microplastics, *ACS Applied Polymer Materials*, Vol.2021, 2021, pp. 4685-4694.

[34] Z. Wang, C. Sun, F. Li, L. Chen, Fatigue Resistance, Re-Useable and Biode Gradable Sponge Materials from Plant Protein with Rapid Water Adsorption Capacity for Microplastics Removal, *Chemical Engineering Journal*, Vol.415, 2021, 129006.

[35] C. Sun, Z. Wang, H. Zheng, L. Chen, F. Li, Biodegradable and Re-useable Sponge Materials Made from Chitin for Efficient Removal of Microplastics, *Journal of Hazardous Materials*, Vol.420, 2021, 126599.

[36] F. Yuan, L. Yue, H. Zhao, H. Wu, Study on the Adsorption of Polystyrene Microplastics by Three-dimensional Reduced Graphene Oxide, *Water Science and Technology*, Vol.81, No.10, 2020, pp. 2163-2175.

[37] J. Wang, C. Sun, Q.X. Huang, Y. Chi, J.H. Yan, Adsorption and Thermal Degradation of Microplastics from Aqueous Solutions by Mg/Zn Modified Magnetic Biochars, *Journal of Hazardous Materials*, Vol.419, 2021, 126486.

[38] K. Kuoppamaki, S. Pflugmacher Lima, C. Scopetani, H. Setala, The Ability of Selected Filter Materials in Removing Nutrients, Metals, and Microplastics from Stormwater in Biofilter Structures, *Journal of Environmental Quality*, Vol.50, No.2, 2021, pp. 465-475.

[39] M. Shen, Y. Zhang, E. Almatrafi, T. Hu, C. Zhou, B. Song, Z. Zeng, G. Zeng, Efficient Removal of Microplastics from Wastewater by an Electrocoagulation Process, *Chemical Engineering Journal*, Vol.428, 2022, 131161.

[40] Z. Chen, W. Wei, X. Liu, B.-J. Ni, Emerging Electrochemical Techniques for Identifying and Removing Micro/Nanoplastics in Urban Waters, *Water Research*, Vol.221, 2022, 118846.

[41] M. Peydayesh, T. Suta, M. Usuelli, S. Handschin, G. Canelli, M. Bagnani, R. Mezzenga, Sustainable Removal of Microplastics and Natural Organic Matter from Water by Coagulation-Flocculation with Protein Amyloid Fibrils, *Environmental Science and Technology*, Vol.55, No.13, 2021, pp. 8848-8858.

[42] P.T. Chazovachii, J.M. Rieland, V.V. Sheffey, Timothy M.E. Jugovic, P. Zimmerman, O. Eniola-Adefeso, B. Love, A. McNeil, Using Adhesives to Capture Microplastics from Water, *American Chemical Society Environmental Science and Technology Engineering*, Vol.1, No.12, 2021, pp. 1698-1704.

[43] P. Wang, Z. Huang, S. Chen, M. Jing, Z. Ge, J. Chen, S. Yang, J. Chen, Y. Fang, Sustainable Removal of Nano/Microplastics in Water by Solar Energy, *Chemical Engineering Journal*, Vol.428, 2022, 131196, pp.1-7.

[44] S.J. Varjani, Microbial Degradation of Petroleum Hydrocarbons, *Bioresource Technology*, Vol.223, 2017, pp. 277–286.

[45] E. Lee, P.R. Rout, J. Bae, The Applicability of Anaerobically Treated Domestic Wastewater as a Nutrient Medium in Hydroponic Lettuce Cultivation: Nitrogen Toxicity and Health Risk Assessment, *Science of the Total Environment*, Vol.780, 2021, 146482.

[46] T. Shindhal, P. Rakholiya, S. Varjani, A. Pandey, H.H. Ngo, W. Guo, M.J. Taherzadeh, A Critical Review on Advances in the Practices and Perspectives for the Treatment of Dye Industry Wastewater, *Bioengineered*, Vol.12, No.1, 2021, pp. 70-87.

[47] P. Torena, M. Alvarez-Cuenca, M. Reza, Biodegradation of Polyethylene Terephthalate Microplastics by Bacterial Communities from Activated Sludge, *The Canadian Journal of Chemical Engineering*, Vol.99, No.S1, 2021, pp. S69-S82.

[48] Z. Chen, W. Zhao, R. Xing, S. Xie, X. Yang, P. Cui, J. Lü, H. Liao, Z. Yu, S. Wang, S. Zhou, Enhanced in Situ Biodegradation of Microplastics in Sewage Sludge Using Hyperthermophilic Composting Technology, *Journal of Hazardous Materials,* Vol.384, 2020, 121271.

[49] A. Tripathi, M.R. Ranjan, Heavy Metal Removal from Wastewater Using Low-Cost Adsorbents, *Journal of Bioremediation & Biodegradation*, Vol. 6, No.6, 2015, 315.

[50] A. Abbas, A.M. Al-Amer, T. Laoui, M.J. Al-Marri, M.S. Nasser, M. Khraisheh, M.A. Atieh, Heavy Metal Removal from Aqueous Solution

by Advanced Carbon Nanotubes: Critical Review of Adsorption Applications, *Separation and Purification Technology*, Vol.157, 2016, pp. 141-161.

[51] Y. Nakano, K. Takeshita, T. Tsutsumi, Adsorption Mechanism of Hexavalent Chromium by Redox within Condensed-Tannin Gel, *Water Research*, Vol.35, No.2, 2001, pp. 496-500.

[52] H. Karimi-Maleh, A. Ayati, S. Ghanbari, Y. Orooji, B. Tanhaei, F. Karimi, M. Alizadeh, J. Rouhi, L. Fu, M. Sillanpää, Recent Advances in Removal Techniques of Cr (VI) Toxic Ion from Aqueous Solution: A Comprehensive Review, *Journal of Molecular Liquids*, Vol.329, 2021, 115062.

[53] C. Sun, Z. Wang, L. Chen, F. Li, Fabrication of Robust and Compressive Chitin and Graphene Oxide Sponges for Removal of Microplastics with Different Functional Groups, *Journal of Chemical Engineering*, Vol.393, 2020, 124796.

[54] P. Risch, C. Adlhart, A Chitosan Nanofiber Sponge for Oyster-Inspired Filtration of Microplastics, *ACS Applied Polymer Materials*, Vol.3, No.9, 2021, pp. 4685-4694.

[55] C. Sun, Z. Wang, H. Zheng, L. Chen, F. Li, Biodegradable and Re-useable Sponge Materials Made from Chitin for Efficient Removal of Microplastics, *Journal of Hazardous Materials*, Vol.420, 2021, 126599.

[56] Z. Wang, C. Sun, F. Li, L. Chen, Fatigue Resistance, Re-Useable and Biodegradable Sponge Materials from Plant Protein with Rapid Water Adsorption Capacity for Microplastics Removal, *Chemical Engineering Journal*, Vol.415, 2021, 129006.

[57] F. Yuan, L. Yue, H. Zhao, H. Wu, Study on the Adsorption of Polystyrene Microplastics by Three-Dimensional Reduced Graphene Oxide, *Water Science and Technology*, Vol.81, No.10, 2020, pp. 2163-2175.

[58] J. Wang, C. Sun, Q.X. Huang, Y. Chi, J.H. Yan, Adsorption and Thermal Degradation of Microplastics from Aqueous Solutions by Mg/Zn Modified Magnetic Biochars, *Journal of Hazardous Materials*, Vol.419, 2021, 126486.

[59] M. Sun, W. Chen, X. Fan, C. Tian, L. Sun, H. Xie, Cooperative Recyclable Magnetic Microsubmarines for Oil and Microplastics Removal from Water, *Applied Materials Today*, Vol.20, 2020, 100682.

[60] J. Wu, R. Jiang, W. Lin, G. Ouyang, Effect of Salinity and Humic Acid on the Aggregation and Toxicity of Polystyrene Nanoplastics with Different Functional Groups and Charges, *Environmental Pollution*, Vol.245, 2019, pp. 836-843.

[61] J. Yuan, J. Ma, Y. Sun, T. Zhou, Y. Zhao, F. Yu, Microbial Degradation and Other Environmental Aspects of Microplastics/Plastics, *Science of the Total Environment*, Vol.715, 2020, 136968.

[62] Z.S. Iro, C. Subramani, S. Dash, A Brief Review on Electrode Materials for Supercapacitor, *International Journal of Electrochemical Science*, Vol.11, 2016, pp. 10628-10643.

[63] W. Zhang, H. Cheng, Q. Niu, M. Fu, H. Huang, D. Ye, Microbial Targeted Degradation Pretreatment: A Novel Approach to Preparation of Activated Carbon with Specific Hierarchical Porous Structures, High Surface Areas, and Satisfactory Toluene Adsorption Performance, *Environmental Science & Technology,* Vol.53, No.13, 2019, pp. 7632−7640.

[64] H. Ge, J. Wang, Ear-like Poly (acrylic acid)-activated Carbon Nanocomposite: A Highly Efficient Adsorbent for Removal of Cd (II) from Aqueous Solutions, *Chemosphere*, Vol.169, 2017, pp. 443-449.

[65] Y.-Y. Zhang, Q. Liu, C. Yang, S.-C. Wu, J.-H. Cheng, Magnetic Aluminum-Based Metal Organic Framework as a Novel Magnetic Adsorbent for the Effective Removal of Minocycline from Aqueous Solutions, *Environmental Pollution*, Vol.255, No.2, 2019, 113226.

[66] B. Peng, T. Song, T. Wang, L. Chai, W. Yang, X. Li, C. Li, H. Wang, Facile Synthesis of Fe_3O_4@$Cu(OH)_2$ Composites and Their Arsenic Adsorption Application, *Chemical Engineering Journal*, Vol.299, 2016, pp. 15-22.

[67] J. Li, K. Zhang, H. Zhang, Adsorption of Antibiotics on Microplastics, *Environmental Pollution*, Vol.237, 2018, pp. 460-467.

[68] G. Liu, L. Li, D. Xu, X. Huang, X. Xu, S. Zheng, Y. Zhang, H. Lin, Metal–organic Framework Preparation Using Magnetic Graphene Oxide–B-Cyclodextrin for Neonicotinoid Pesticide Adsorption and Removal, *Carbohydrate Polymers*, Vol.175, 2017, pp. 584-591.

[69] B. Aguila, D. Banerjee, Z. Nie, Y. Shin, S. Mab, P.K. Thallapally, Selective Removal of Cesium and Strontium Using Porous Frameworks from high level nuclear waste, *Chemical Communications*, Vol.52, No.35, 2016, pp. 5940-5942.

[70] V. Soni, D.A. Dinh, K. Poonia, R. Kumar, P. Singh, V.K. Ponnusamy, R. Selvasembian, A. Singh, V. Chaudhary, S. Thakur, L.H. Nguyen, L.-A.P. Thi, V.-H. Nguyen, P. Raizada,

Upcycling of Polyethylene Terephthalate (PET) Plastic Wastes into Carbon-Based Nanomaterials: Current Status and Future Perspectives, *European Polymer Journal*, Vol.215, 2024, 113249.

[71] S. Sharifian, N. Asasian-Kolur, Polyethylene Terephthalate (PET) Waste to Carbon Materials: Theory, Methods and Applications, *Journal of Analytical and Applied Pyrolysis*, Vol.163, 2022, 105496.

[72] F. Pasanen, R.O. Fuller, F. Maya, Sequential Extraction, Depolymerization and Quantification of Polyethylene Terephthalate Nanoplastics Using Magnetic ZIF-8 Nanocomposites, *Chemical Engineering Journal*, Vol.490, 2024, 151453.

[73] H. Zheng, Q. Chen, Z. Chen, Carbon-based Adsorbents for Micro/Nano-Plastics Removal: Current Advances and Perspectives, *Water Emerging Contaminants & Nanoplastics*, Vol.3, No.11, 2024, pp.1-15.

[74] H. Kang, A. Washington, M.D. Capobianco, X. Yan, V.V. Cruz, M. Weed, J. Johnson, G. Johns III, G.W. Brudvig, X. Pan, J. Gu, Concentration-Dependent Photocatalytic Upcycling of Poly(ethylene terephthalate) Plastic Waste, *ACS Materials Letters*, Vol.5, No.11, 2023, pp. 3032-3041.

[75] A. Tchinsa, Md. F. Hossain, T. Wang, Y. Zhou, Removal of Organic Pollutants from Aqueous Solution Using Metal Organic Frameworks (MOFs)-based Adsorbents: A Review, *Chemosphere*, Vol.284, 2021, 131393.

[76] A.I.S. Purwiyanto, Y. Suteja, Trisno, P.S. Ningrum, W.A.E. Putri, Rozirwan, F. Agustriani, Fauziyah, M.R. Cordova, A.F. Koropitan, Concentration and Adsorption of Pb and Cu in Microplastics: Case Study in Aquatic Environment, *Marine Pollution Bulletin*, Vol.158, 2020, 111380.

[77] Y. Tang, S. Zhang, Y. Su, D. Wu, Y. Zhao, B. Xie, Removal of Microplastics from Aqueous Solutions by Magnetic Carbon Nanotubes, *Chemical Engineering Journal*, Vol.406, 2021, 126804.

[78] L.M. Tijerina, C.M. Oliva González, B.I. Kharisov, T.E. Serrano Quezada, Y. Peña Méndez, O.V. Kharissova, I. Gómez de la Fuente, Synthesis of MOF-derived Bimetallic Nanocarbons CuNi@C with Potential Applications as Counter Electrodes in Solar Cells, *Mendeleev Communications*, Vol.29, No.4, 2019, pp. 400-402.

[79] X. Huang, X. Zhan, C. Wen, F. Xu, L. Luo, Amino-functionalized Magnetic Bacterial Cellulose/Activated Carbon Composite for Pb^{2+} and Methyl Orange Sorption from Aqueous Solution, *Journal of Materials Science & Technology,* Vol.34, No.5, 2018, pp. 855-863.

[80] D.T. Sponza, R. Öztekin, Methane Production from Carbondioxide in Polluted Areas Using Graphene Doped Ni/NiO Nanocomposite via Photocatalysis, *Advances in Earth and Environmental Science*, Vol.2, No.4, 2021, pp. 1-17.

[81] R. Öztekin, D.T. Sponza, Methane Production from Carbondioxide in Polluted Areas Using Graphene Doped Ni/NiO Nanocomposite via Photocatalytic Degradation Process, *International Journal of Advanced Multidisciplinary Research and Studies*, Vol.3, No.2, 2023, pp. 617-631.

[82] H. Hammani, W. Boumya, F. Laghrib, A. Farahi, S. Lahrich, A. Aboulkas, M. El Mhammedi, Electrocatalytic Effect of NiO Supported onto Activated Carbon in Oxidizing Phenol at Graphite Electrode: Application in Tap Water and Olive Oil Samples, *Journal of the Association of Arab Universities for Basic and Applied Sciences*, Vol.24, 2017, pp. 26-33.

[83] M.S. Yadav, N. Singh, S.M. Bobade, Electrochemical Analysis of CuO-AC Based Nanocomposite for Supercapacitor Electrode Application, *Materials Today: Proceedings*, Vol.28, No.1, 2020, pp. 366−374.

[84] L. Wang, A. Kaeppler, D. Fischer, J. Simmchen, Photocatalytic TiO_2 Micromotors for Removal of Microplastics and Suspended Matter, *ACS Applied Materials & Interfaces*, Vol.11, No.36, 2019, pp. 32937-32944.

[85] K. Villa, L. Dekanovský, J. Plutnar, J. Kosina, M. Pumera, Swarming of Perovskite-like Bi_2WO_6 Microrobots Destroy Textile Fibers under Visible Light, *Advanced Functional Materials*, Vol.30, No.51, 2020, 2007073.

[86] L. Wang, K. Villa, Self-propelled Micro/Nanomotors for Removal of Insoluble Water Contaminants: Microplastics and Oil Spills, *Environmental Science. Nano*, Vol.8, No.12, 2021, pp. 3440-3451.

[87] H. Ye, Y. Wang, X. Liu, D. Xu, H. Yuan, H. Sun, S. Wang, X. Ma, Magnetically Steerable Iron Oxides-Manganese Dioxide Core-Shell Micromotors for Organic and Microplastic Removals, *Journal of Colloid and Interface Science*, Vol.588, 2021, pp. 510-521.

[88] A.E. Burakov, E.V. Galunin, I.V. Burakova, A.E. Kucherova, S. Agarwal, A. G. Tkachev, V.K. Gupta, Adsorption of Heavy Metals on Conventional and Nanostructured Materials for

Wastewater Treatment Purposes: A Review, *Ecotoxicology and Environmental Safety*, Vol.148, 2018, pp. 702-712.

[89] W.S. Chai, J.Y. Cheun, P.S. Kumar, M. Mubashir, Z. Majeed, F. Banat, S.-H. Ho, P.L. Show, A Review on Conventional and Novel Materials Towards Heavy Metal Adsorption in Wastewater Treatment Application, *Journal of Cleaner Production*, Vol.296, 2021, 126589.

[90] N. Tiwari, D. Santhiya, J.G. Sharma, Microbial Remediation of Micro-Nano Plastics: Current Knowledge and Future Trends, *Environmental Pollution*, Vol.265, No.Pt A, 2020, 115044.

[91] C.M.R. Almeida, E. Manjate, S. Ramos, Adsorption of Cd and Cu to Different Types of Microplastics in Estuarine Salt Marsh Medium, *Marine Pollution Bulletin*, Vol.151, 2020, 110797.

[92] P.U. Iyare, S.K. Ouki, T. Bond, Microplastics Removal in Wastewater Treatment Plants: A Critical Review, *Environmental Science: Water Research & Technology*, Vol.6, No.10, 2020, pp. 2664–2675.

[93] S. Yang, L. Li, Z. Pei, C. Li, J. Lv, J. Xie, B. Wen, S. Zhang, Adsorption Kinetics, Isotherms and Thermodynamics of Cr (III) on Graphene Oxide, *Colloids and Surfaces A: Physicochemical and Engineering Aspects*, Vol.457, 2014, pp. 100–106.

[94] Y.G. Wibowo, H. Safitri, B.S. Ramadan, Adsorption Test Using Ultra-Fine Materials on Heavy Metals Removal, *Bioresource Technology Reports*, Vol.19, 2022, 101149.

[95] S.A. Sadeek, N.A. Negm, H.H. Hefni, M.M. Abdel Wahab, Metal Adsorption by Agricultural Biosorbents: Adsorption Isotherm, Kinetic and Biosorbents Chemical Structures, *International Journal of Biological Macromolecules*, Vol.81, 2015, pp. 400–409.

[96] D.L. Sparks, B. Singh, M.G. Siebecker, Chapter 5 - *Sorption Phenomena on Soils. In Environmental Soil Chemistry* (Third Edition), Sparks, D. L.; Singh, B.; Siebecker, M. G., Eds. Academic Press: Boston, 2023; pp 203-281.

[97] J.H. Zar, *Biostatistical Analysis*, Prentice-Hall, Englewood Cliffs, New Jersey, USA, 1984.

[98] Statgraphics Centurion XV, sofware, StatPoint Inc, Statgraphics Centurion XV, Herndon, VA, USA, 2005.

[99] S.D. Afonnikova, I.V. Mishakov, Y.I. Bauman, M.V. Trenikhin, Y.V. Shubin, A.N. Serkova, A.A. Vedyagin, Preparation of Ni–Cu Catalyst for Carbon Nanofiber Production by the Mechanochemical Route, *Topics in Catalysis*, Vol.66, 2022, pp. 393–404.

[100] S.M. Mintenig, I. Int-Veen, M.G. Loder, S. Primpke, G. Gerdts, Identification of Microplastic in Effluents of Wastewater Treatment Plants Using Focal Plane Array-based Micro-Fourier-transform Infrared Imaging, *Water Research*, Vol.108, 2017, pp. 365-372.

[101] S. Xu, J. Ma, R. Ji, K. Pan, A.J. Miao, Microplastics in Aquatic Environments: Occurrence, Accumulation, and Biological Effects, *Science of the Total Environment*, Vol.703, 2019, 134699.

[102] Y.I. Bauman, I.V. Mishakov, A.A. Vedyagin, S. Ramakrishna, Synthesis of Bimodal Carbon Structures via Metal Dusting of Ni-based Alloys. Materials letters, Vol.201, 2017, pp. 70–73.

[103] A.A. Popov, S.D. Afonnikova, A.D. Varygin, Y.I. Bauman, M.V. Trenikhin, P.E. Plyusnin, Y.V. Shubin, A.A. Vedyagin, I.V. Mishakov, I.V. Pt1 xNix Alloy Nanoparticles Embedded in Self-Grown Carbon Nanofibers: Synthesis, Properties and Catalytic Activity in HER, *Catalysts*, Vo.13, No.3, 2023, 599.

[104] J. Zou, X. Liu, D. Zhang, X. Yuan, Adsorption of Three Bivalent Metals by Four Chemical Distinct Microplastics, *Chemosphere*, Vol.248, 2020, 126064.

[105] X. Guo, G. Hu, X. Fan, H. Jia, Sorption Properties of Cadmium on Microplastics: The Common Practice Experiment and a Two-Dimensional Correlation Spectroscopic Study, *Ecotoxicology and Environmental Safety*, Vol.190, 2020, 110118.

[106] L. Lin, S. Tang, X. Wang, X. Sun, A. Yu, Hexabromocyclododecane Alters Malachite Green and Lead(II) Adsorption Behaviors Onto Polystyrene Microplastics: Interaction Mechanism And Competitive Effect, *Chemosphere*, Vol.265, 2021, 129079.

[107] Z. Lin, Y. Hu, Y. Yuan, B. Hu, B. Wang, Comparative Analysis of Kinetics and Mechanisms for Pb(II) Sorption onto Three Kinds of Microplastics, *Ecotoxicology and Environmental Safety*, Vol.208, 2021, 111451.

[108] A.I.S. Purwiyanto, Y.T. Suteja, P.S. Trisno; Ningrum, W.A.E. Putri, Rozirwan, F. Agustriani, F. Fauziyah, M.R. Cordova, A.F. Koropitan, Concentration and Adsorption of Pb and Cu in Microplastics: Case Study in Aquatic Environment, *Marine Pollution Bulletin*, Vol.158, 2020, 111380.

[109] S. Tang, L. Lin, X. Wang, A. Feng, A. Yu, Pb(II) Uptake onto Nylon Microplastics: Interaction Mechanism and Adsorption

Performance, Journal of. Hazardous Materials, Vol.386, 2020, 121960.

[110] Q. Wang, Y. Zhang, X. Wangjin, Y. Wang, G. Meng, Y. Chen, The Adsorption Behavior of Metals in Aqueous Solution by Microplastics Effected by UV Radiation, Journal of *Environmental Science International*, Vol.87, 2020, pp. 272–280.

[111] P. Zhou, M. Adeel, N. Shakoor, M. Guo, Y. Hao, I. Azeem, M. Li, M. Liu, Y. Rui, Application of Nanoparticles Alleviates Heavy Metals Stress and Promotes Plant Growth: An Overview, *Nanomaterials,* Vol.11, No.1, 2020, 26.

Contribution of Individual Authors to the Creation of a Scientific Article (Ghostwriting Policy)

Prof. Dr. Delia Teresa Sponza and Post-Dr. Rukiye Öztekin took an active role in every stage of the preparation of this article.

The authors equally contributed in the present research, at all stages from the formulation of the problem to the final findings and solution.

Sources of Funding for Research Presented in a Scientific Article or Scientific Article Itself

The experimental phases of this research study were conducted at the National Research Council (NRC) of Canada, Research Centres, Ontario, Canada. The authors would like to thank this body for providing financial support.

Conflict of Interest

The authors have no conflicts of interest to declare that are relevant to the content of this article.

APPENDIX

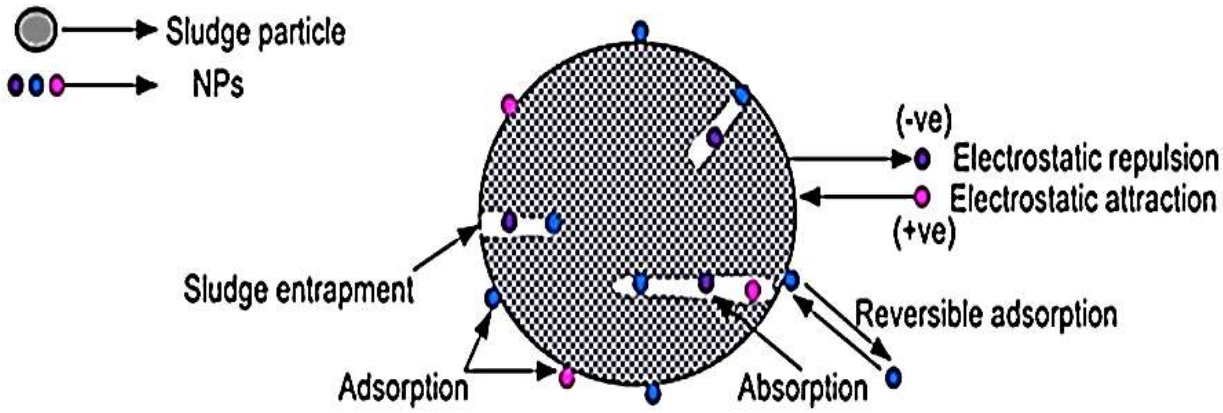

Fig. 1. Mechanism of sorption of NPs removal during ASP in wastewater treatment plants.

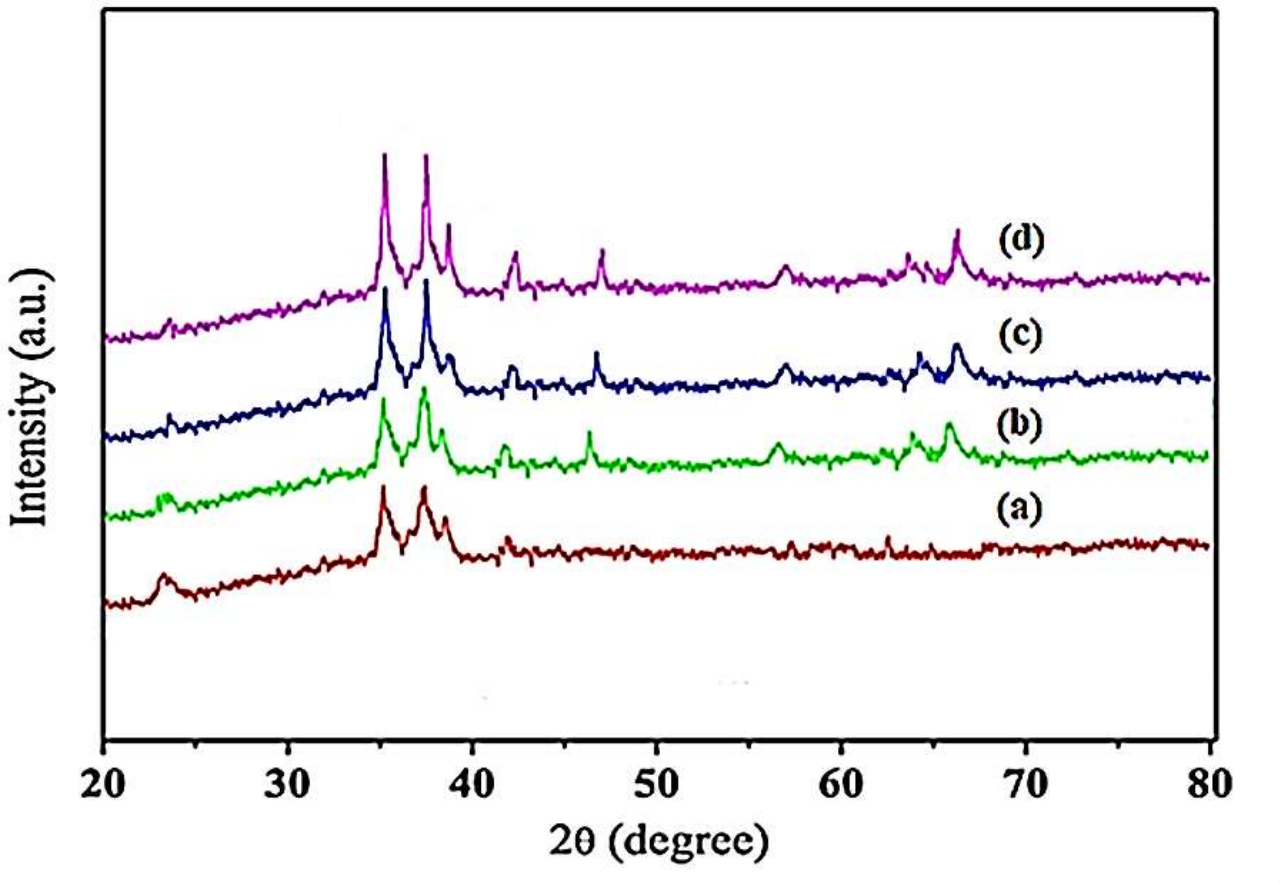

Fig. 2. XRD spectrum of Ni-Cu-C NCs **(a)** after 30 min (red spectra), **(b)** after 60 min (green spectra), **(c)** after 90 min (blue spectra) and **(d)** after 120 min (pink spectra) adsorption times, respectively, in an activated sludge solution with adsorption process for PET NPs removal.

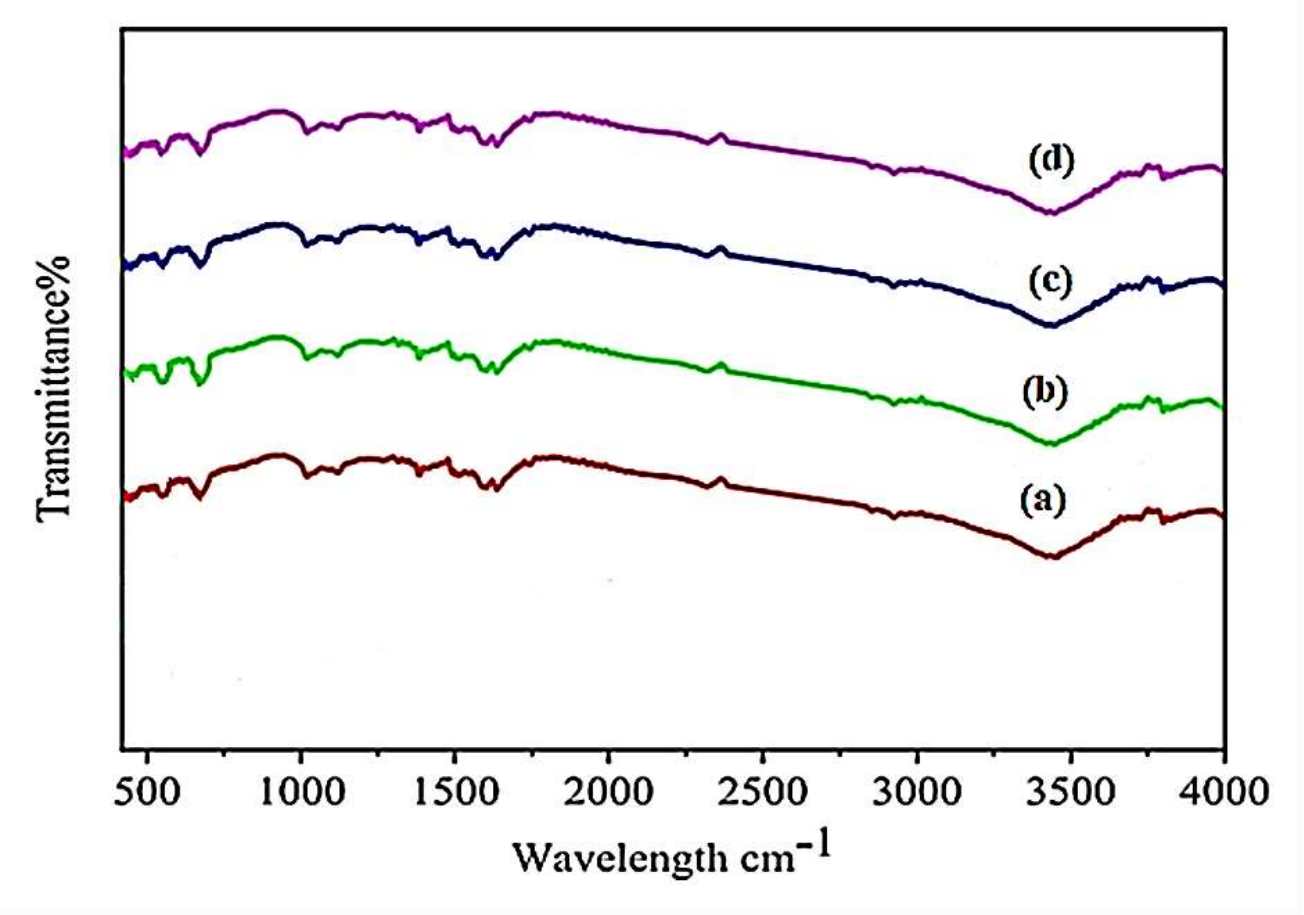

Fig. 3. FTIR spectrum of Ni-Cu-C NCs **(a)** after 30 min (red spectra), **(b)** after 60 min (green spectra), **(c)** after 90 min (blue spectra) and **(d)** after 120 min (pink spectra), respectively, in an activated sludge solution with adsorption process for PET NPs removal.

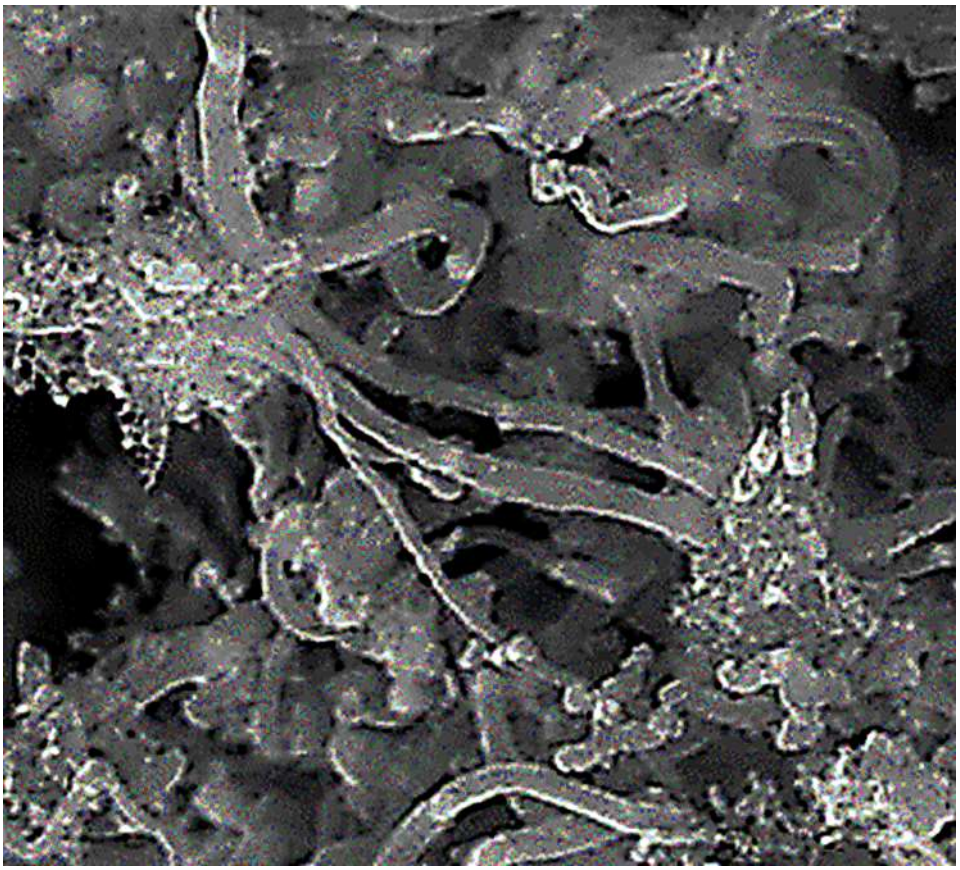

Fig. 4. FESEM images of Ni-Cu-C NCs in an activated sludge solution with adsorption process for PET NPs removal after 120 adsorption time (FESEM image size: 1μm).

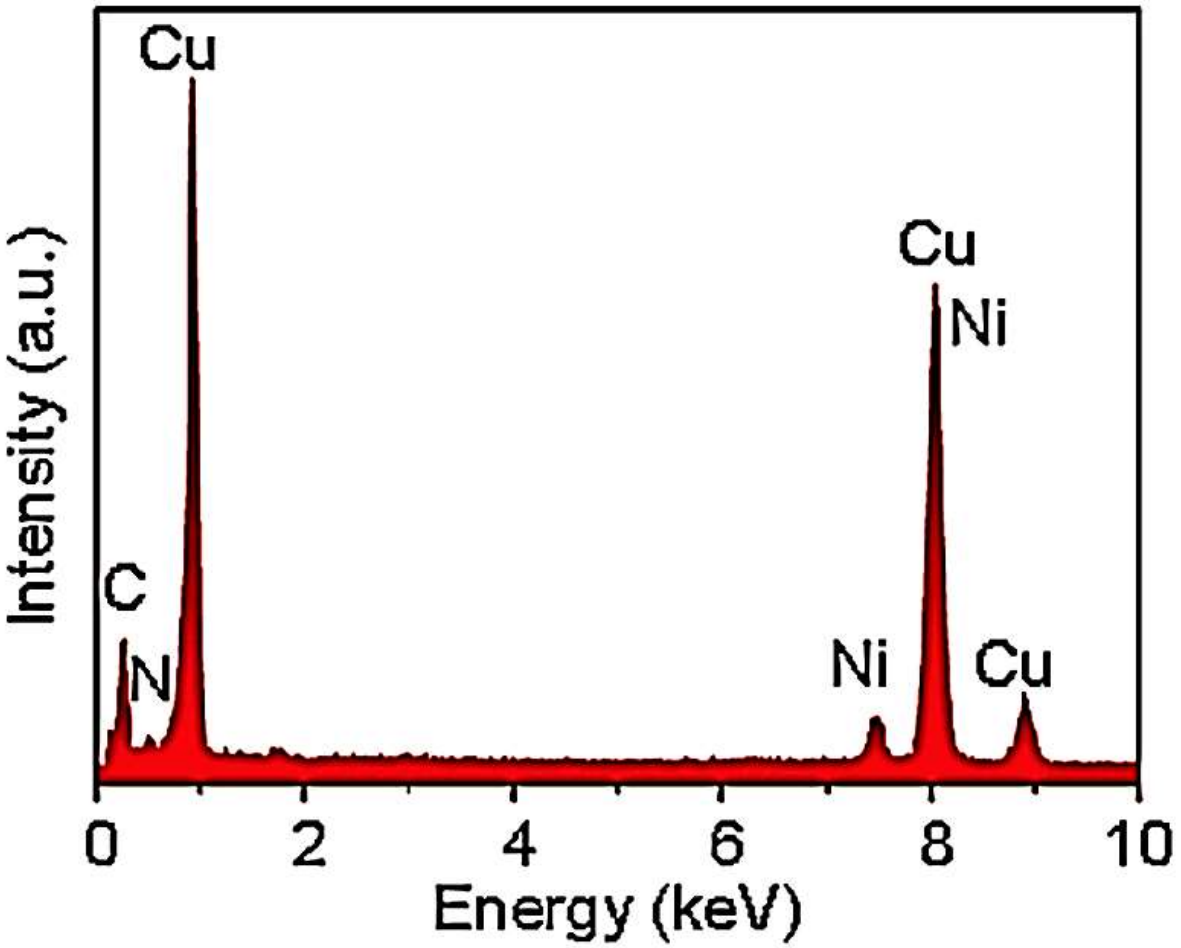

Fig. 5. EDX images of Ni-Cu-C NCs in an activated sludge solution with adsorption process for PET NPs removal.

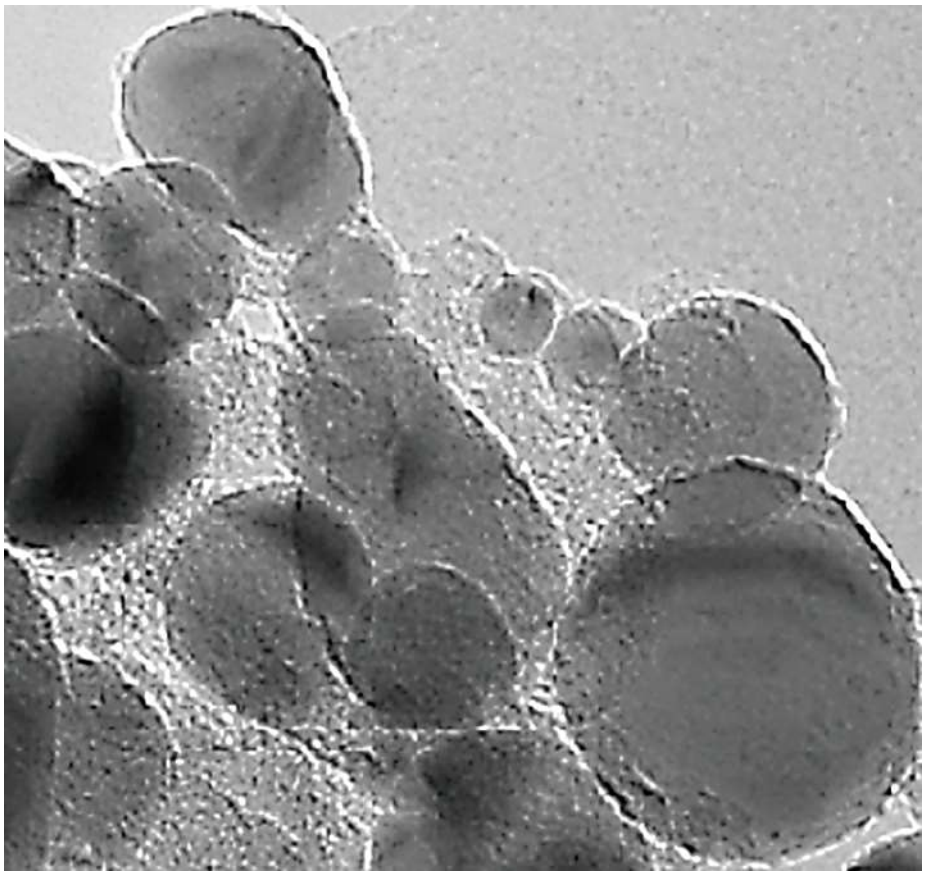

Fig. 6. HRTEM images of Ni-Cu-C NCs in micromorphological structure level in an activated sludge solution with adsorption process for PET NPs removal after 120 min adsorption time (HRTEM image size: 1μm).

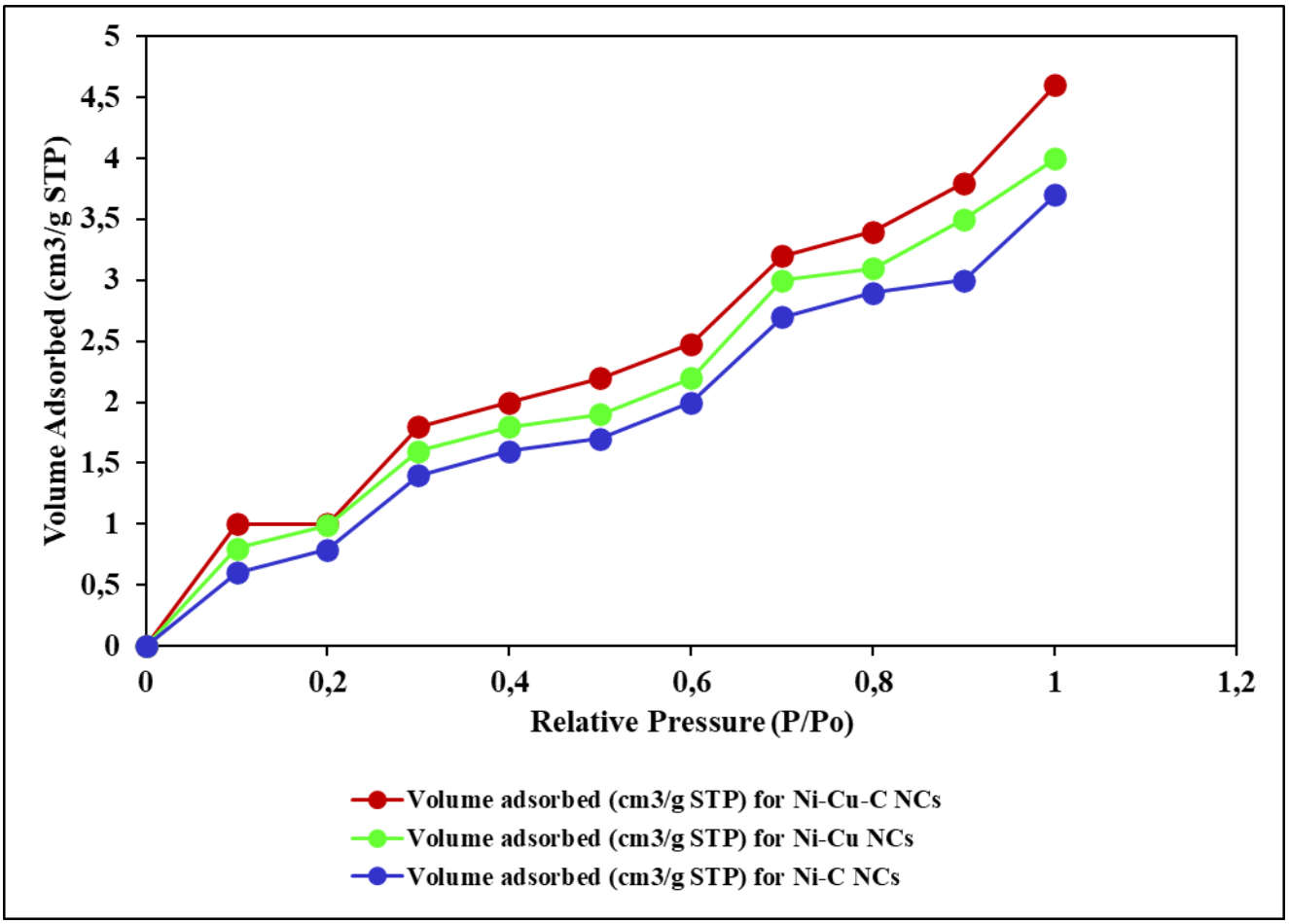

Fig. 7a. N_2 Adsorption/Desorption of Ni-Cu-C NCs

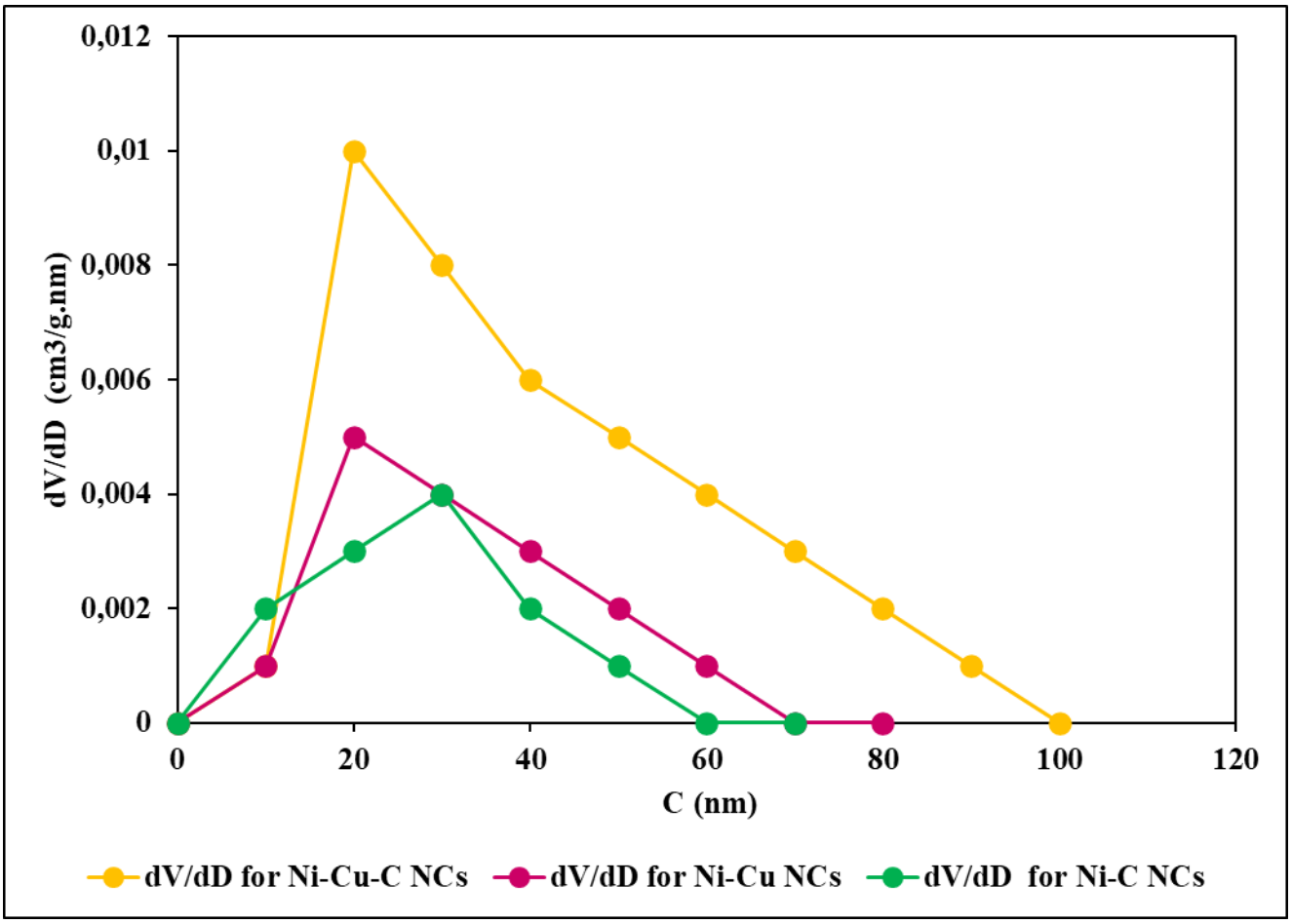

Fig. 7b. BJH por size distribution of Ni-Cu-C, Ni-C and Ni-C NCs

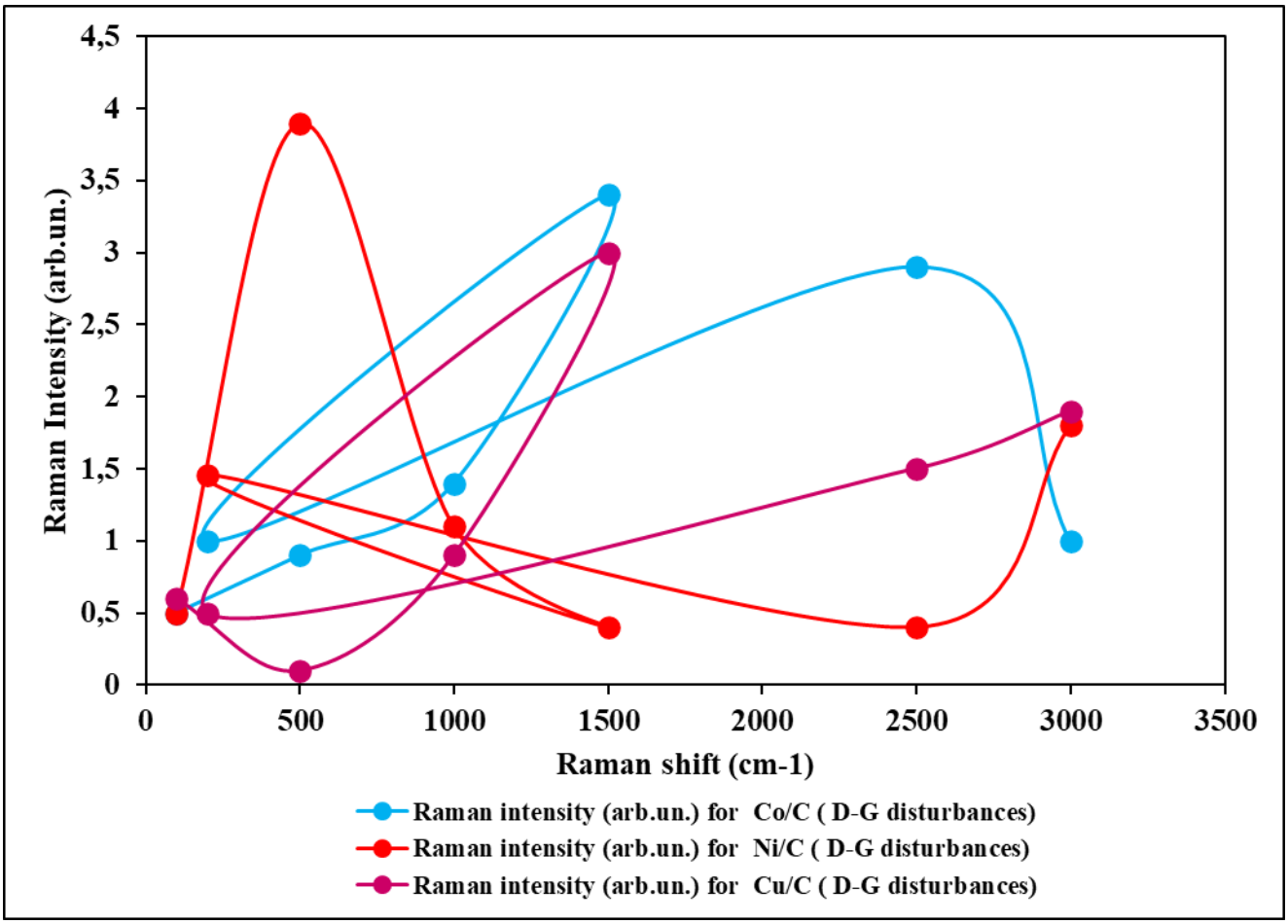

Fig. 8. Raman Streptoscopy analysis results

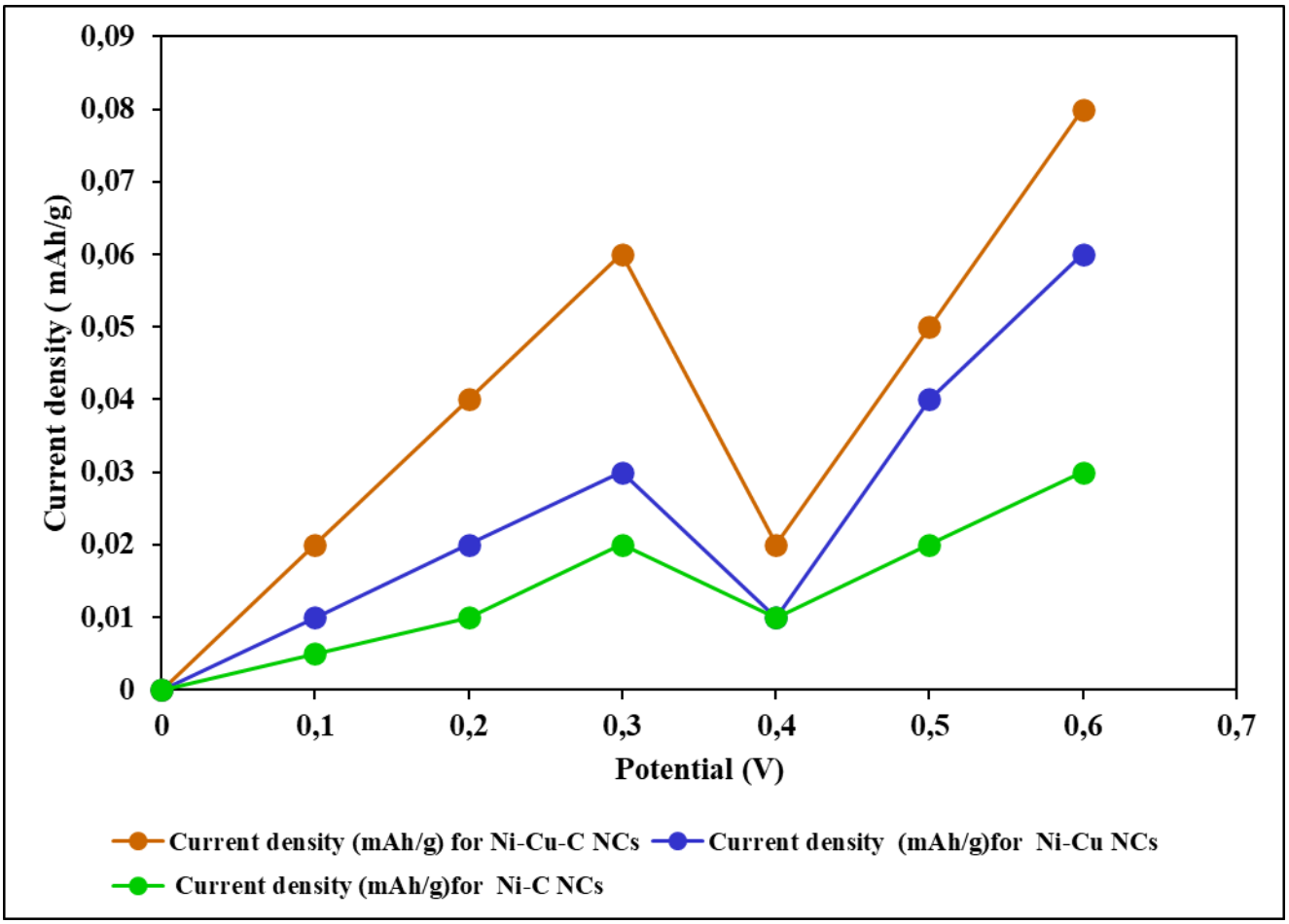

Fig. 9. CV curves of Ni-Cu-C NCs

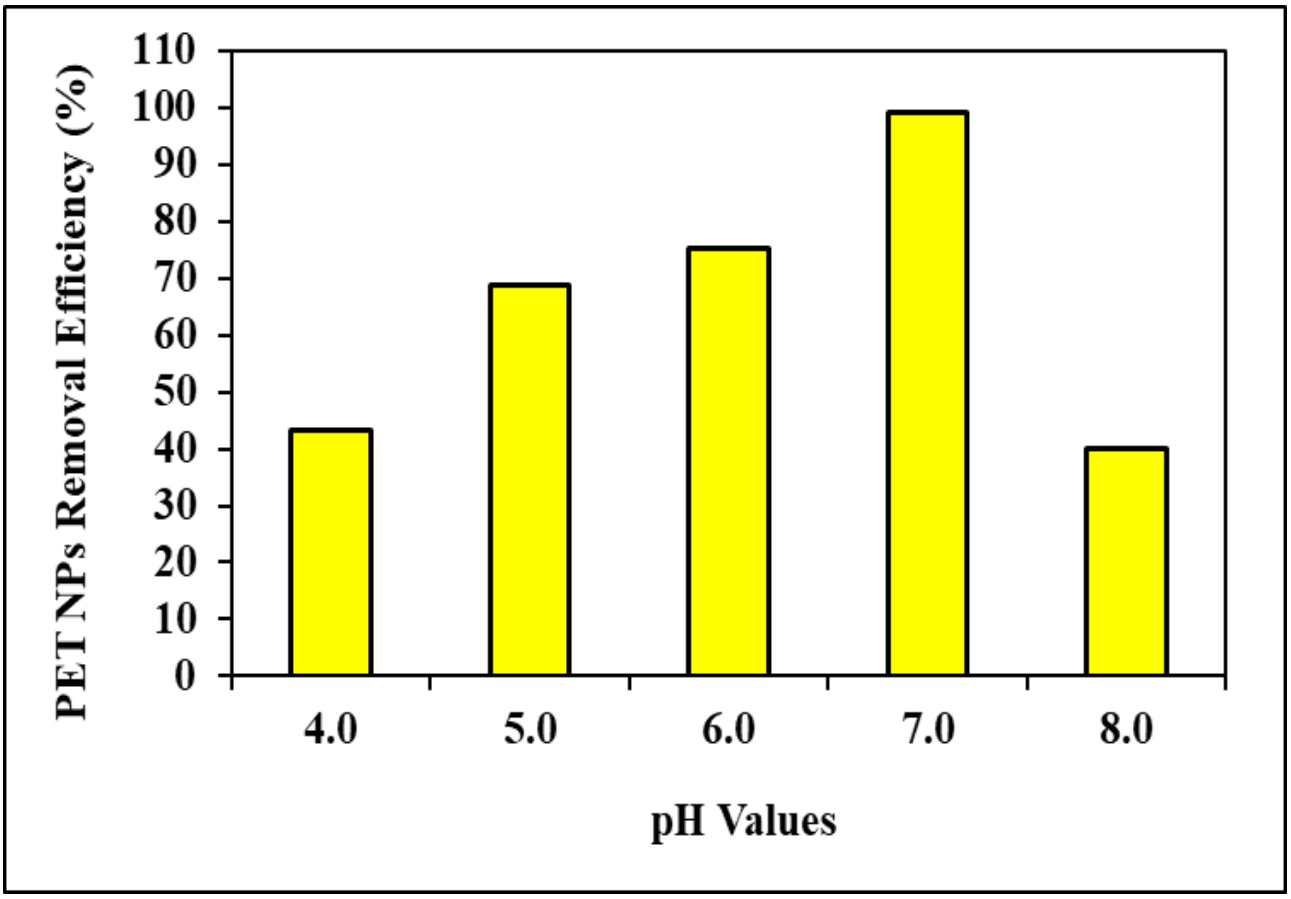

Fig. 10. Effect of increasing pH values in an activated sludge solution during adsorption process for PET NPs removal, at 25ºC.

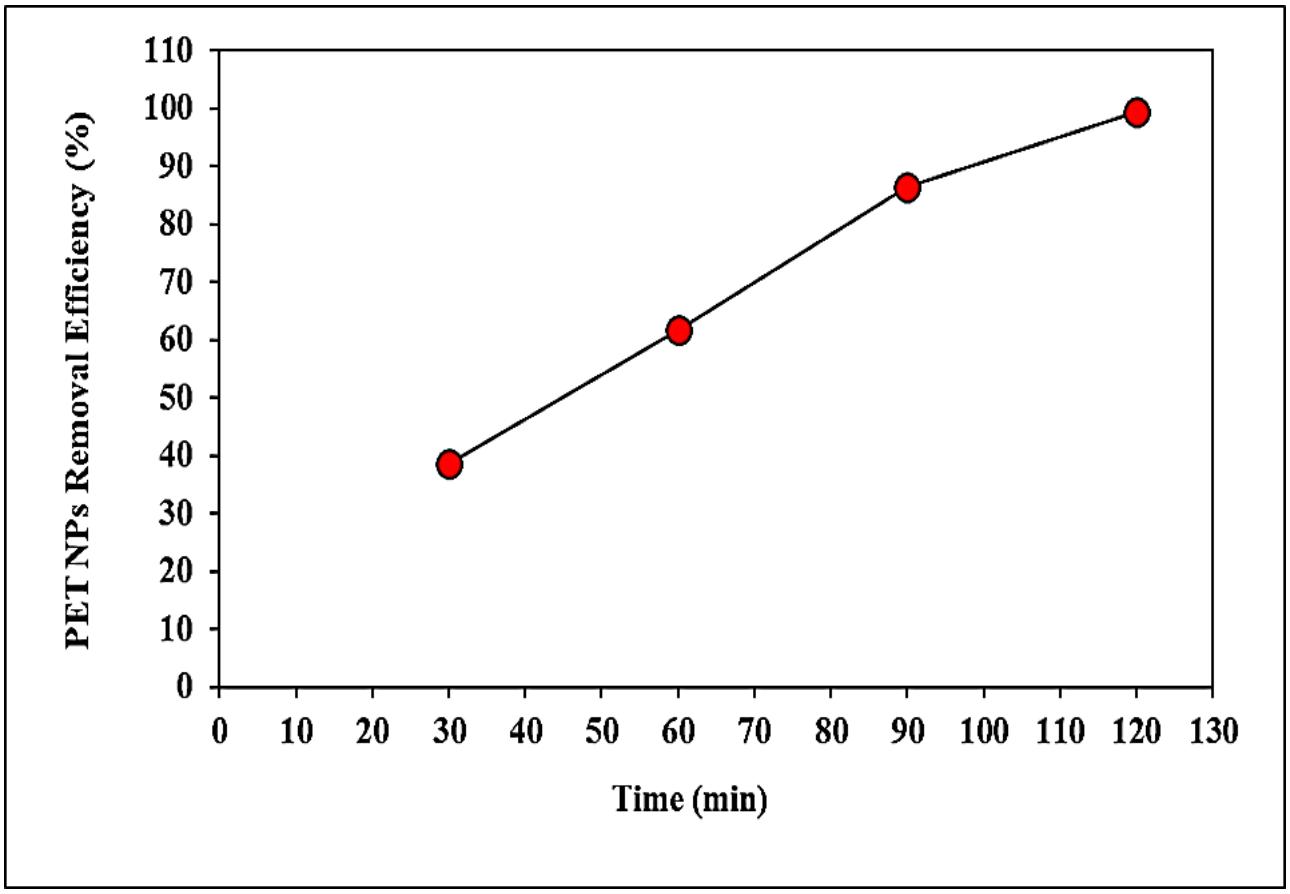

Fig. 11. Effect of increasing adsorption times in an activated sludge solution during adsorption process for PET NPs removal, at pH=5.0 and at 25ºC.

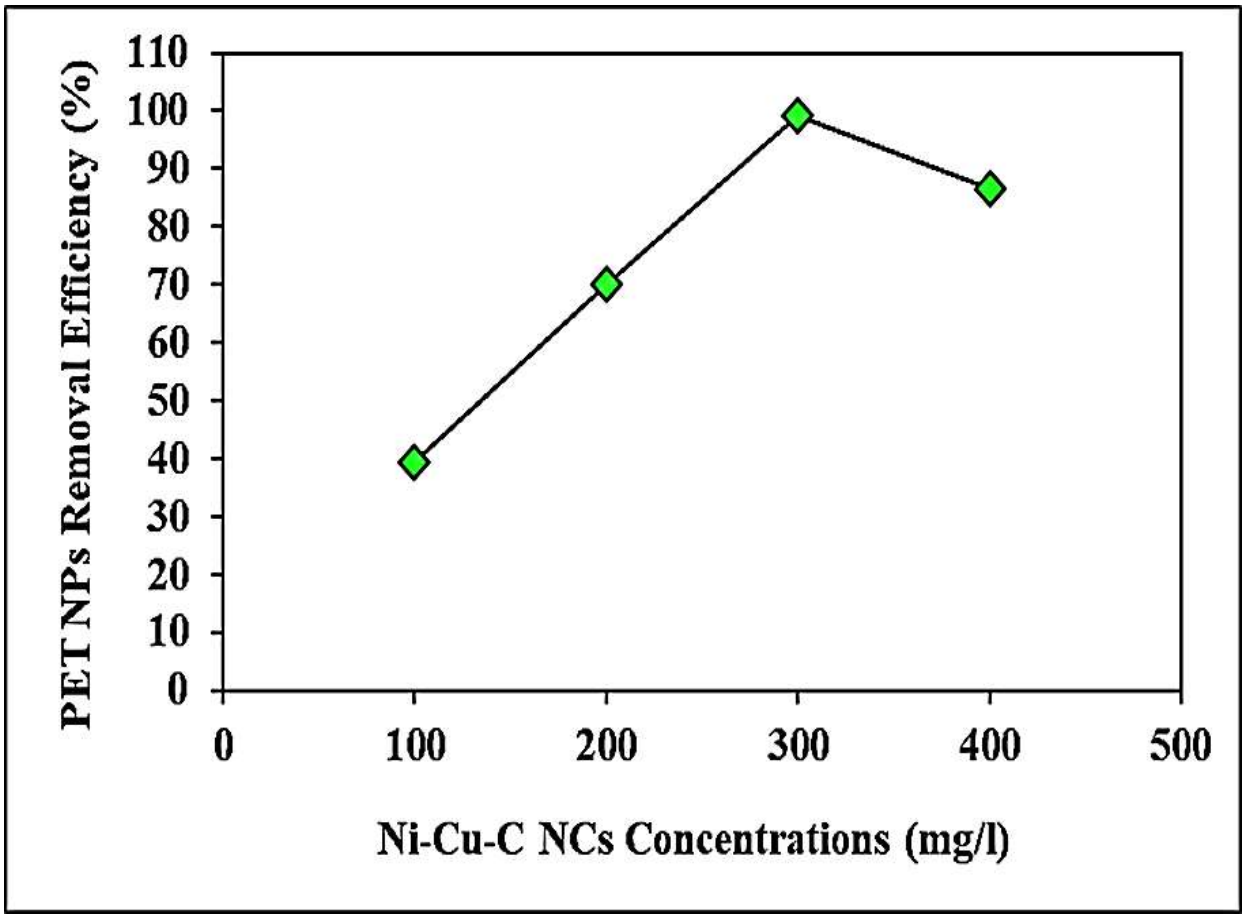

Fig. 12. Effect of increasing Ni-Cu-C NCs adsorbent concentrations in an activated sludge solution during adsorption process for PET NPs removal, after 120 min adsorption time, at pH=5.0 and at 25°C.

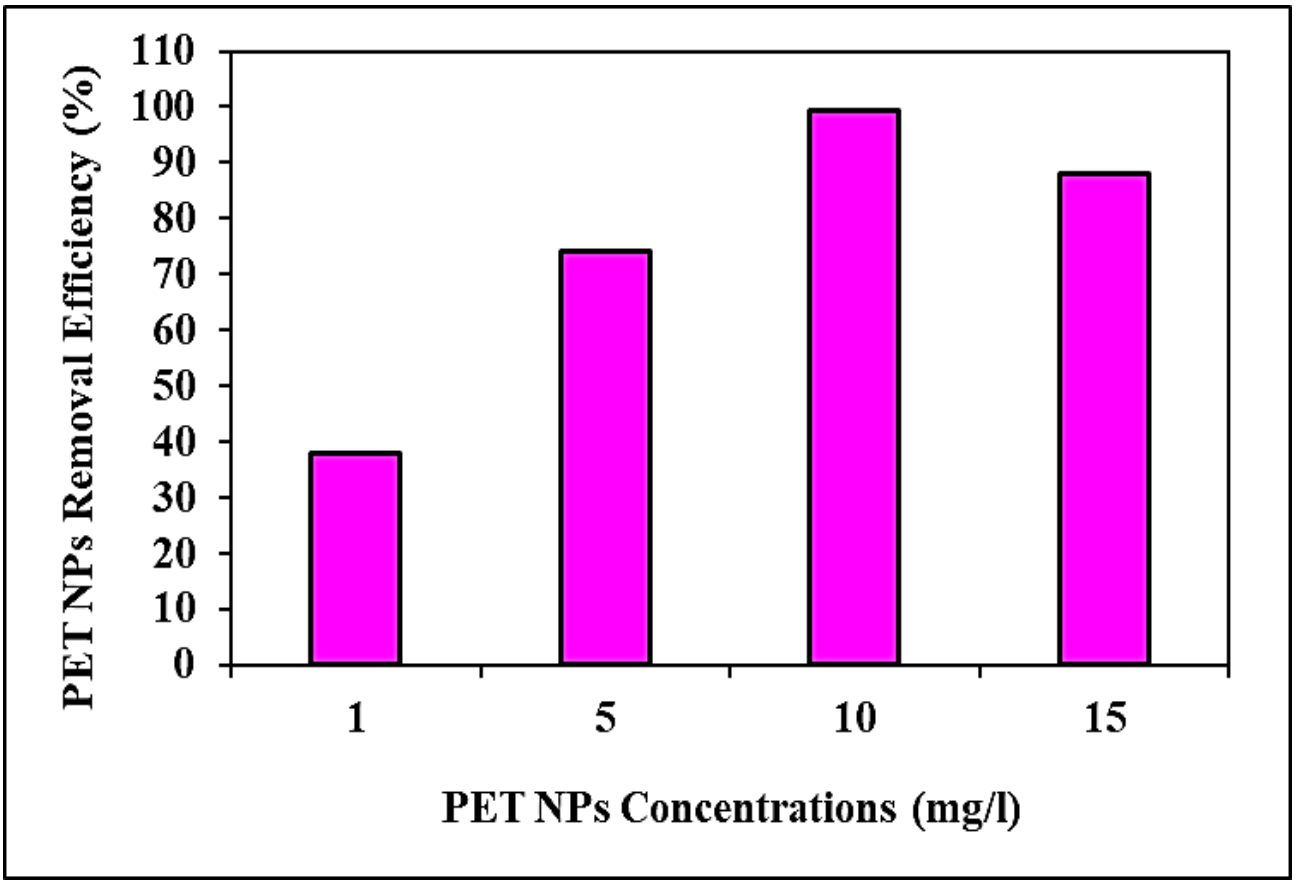

Fig. 13. Effect of increasing PET NPs concentrations in an activated sludge solution during adsorption process for PET NPs removal, after 120 min adsorption time, at pH=5.0 and at 25°C.